STUDIES IN PATHOGENESIS OF A NOVEL ISOLATE OF *CRONOBACTER SAKAZAKII* USING AN *IN VITRO* BLOOD BRAIN BARRIER MODEL

A Thesis
Submitted to the Graduate Faculty
of the
North Dakota State University
of Agriculture and Applied Science

By

Elliott Weston Welker

In Partial Fulfillment
for the Degree of
MASTER OF SCIENCE

Major Program:
Microbiology

August 2013

Fargo, North Dakota

North Dakota State University
Graduate School

STUDIES IN PATHOGENESIS OF A NOVEL ISOLATE OF *CRONOBACTER SAKAZAKII* USING AN *IN VITRO* BLOOD BRAIN BARRIER MODEL

By

Elliott Weston Welker

The Supervisory Committee certifies that this ***disquisition*** complies with North Dakota State University's regulations and meets the accepted standards for the degree of

MASTER OF SCIENCE

SUPERVISORY COMMITTEE:

Penelope Gibbs
Chair

Nathan Fisher

Birgit Pruess

Neil Dyer

Anne Denton

Approved:

February 24, 2014
Date

Charlene Wolf-Hall
Department Chair

ABSTRACT

Genus *Cronobacter* is a member of the family *Enterobacteriaceae* consisting of several opportunistic species. The primary focus of this study was to utilize an *in vitro* co-culture model of the blood brain barrier to investigate a bovine fecal strain of *C. sakazakii* to investigate pathogenicity. The strain was found to have the same effect on the barrier's integrity as the positive *Escherichia coli* control. Additionally, *C. sakazakii* strain BAA-894 was found to have the same effect as the negative *E. coli* control.

This study also focused on the development of a site-specific mutagenesis procedure for *C. sakazakii.* A procedure using linear transformation was able to replace the putative virulence gene *zpx* (zinc-containing metalloprotease) in *C. sakazakii*. A future virulence study would involve using this mutagenesis procedure to induce a mutation in genes of *C. sakazakii* speculated to play a role in BBB translocation followed by challenge in the BBB model.

ACKNOWLEDGEMENTS

First and foremost, I would like to thank my committee chair Dr. Penelope Gibbs, whose continual guidance and support made this voyage possible. Her wisdom, mentorship style, and belief in my abilities helped me to explore strange new ideas, to seek out new procedures, and to try them even though I had never done them before. Thank you for everything, Captain.

I would like to express my appreciation to my committee members, Dr. Anne Denton, Dr. Neil Dyer, Dr. Nathan Fisher, and Dr. Birgit Pruess for their attentiveness, encouragement, and insight. I would also like to thank my lab manager, Heather Vinson, for always taking the time to help me when I was confused and for answering my many inane questions.

Additionally, I would like to express my gratitude towards Dr. Curt Doetkott for his statistical assistance and the comradeship of my fellow graduate students. And lastly, I would like to thank my fiancée Laura Nessa. Her never ending support and encouragement helped make this research possible.

TABLE OF CONTENTS

LIST OF TABLES

LIST OF FIGURES

LIST OF APPENDIX TABLES

LIST OF APPENDIX FIGURES

INTRODUCTION

The genus *Cronobacter*, of the family *Enterobacteriaceae*, consists of both commensal and opportunistic pathogens. Bacteria of this genus were initially classified as *Enterobacter sakazakii*, but following extensive genetic analysis, including 16S rRNA sequencing, concluded that the entire species should be reorganized into its own unique genus of '*Cronobacter'* [1, 2]. Currently, the genus *Cronobacter* is divided into ten distinct species [3, 4].

Cronobacter spp. has been reported to cause necrotizing enterocolitis (NEC), sepsis, and meningitis in neonates and premature infants [5, 6]. Diseases caused by members of this genus have also been documented in adults, albeit less frequently. Mortality rates in newborns range from 40-80% and tend to receive the majority of research attention while disease in adults may be underreported [7, 8]. The majority of newborn *Cronobacter* infections have been traced back to contaminated powdered infant formula (PIF) as the causative agent [6, 9-11]. The natural reservoir of this genus has not yet been identified, with species being isolated from a number of different food products, environmental sources, and clinical specimens [12-15]. Recent studies have implicated plant roots in the soil as being the likely natural reservoir [16, 17].

Currently, the pathogenic mechanism and virulence factors of *Cronobacter spp.* remain largely undefined. As a member of the family *Enterobacteriaceae*, *Cronobacter* possesses the lipid A core endotoxin on their lipopolysaccharide (LPS). The endotoxin is heat stable and has been shown to remain biologically active in the heat-treated PIF [18]. A study using a suckling mouse model found that LPS plays a role in allowing the bacteria to penetrate the blood brain barrier (BBB) and cause meningitis [19].

Several species of *Cronobacter* are able to invade and translocate across human epithelial colorectal adenocarcinoma (Caco-2) cells and human brain microvascular endothelial cells

(HBMEC) [20]. Two distinct bacterial adhesion patterns have been observed on the eukaryotic cell surfaces: a diffuse pattern and a localized pattern [21]. Invasion of *Cronobacter* has also been attributed in part to an outer membrane protein A (OmpA) in some species, a protein common in many Gram-negative bacteria [22]. The OmpA protein has been shown to play a key role in *Escherichia coli* K1's ability to cause neonatal meningitis [23-25]. Additional studies found that *Cronobacter spp.* contain a plasminogen activator (Cpa) that may aid in serum survival as well as a unique zinc-containing metalloprotease (Zpx) that may play a role in cell barrier disruption [26, 27]. Further investigation into each of these putative virulence factors is needed to determine their role in *Cronobacter's* ability to attach and invade Eukaryotic cells.

This study will focus on *C. sakazakii's* ability to disrupt the cells that comprise the BBB. Many *in vitro* systems used to investigate disruption of the BBB rely on mono-culture models of HBMEC [21]. We propose a co-culture model utilizing mouse endothelial and astrocyte cells in order to more accurately represent the cell-to-cell interactions found in the actual BBB. The integrity of the cellular barrier will be measured using trans-endothelial electrical resistance (TEER). As research into the virulence of this genus is limited, a quick and cost effective procedure for inducing site-specific mutations has yet to be developed. Therefore, this study also proposes a novel method for creating site-specific mutations in putative virulence genes of *C. sakazakii.* This site-specific mutagenesis procedure could potentially be used in conjunction with the co-culture BBB model to investigate putative virulence genes of *C. sakazakii's* translocation across the BBB.

OBJECTIVES

The objectives of this study include:

1. Utilize an *in vitro* co-culture model as a representation of the blood brain barrier (BBB) that consists of secondary mouse endothelial and astrocyte cells to evaluate how various *Cronobacter sakazakii* strains affect the barrier's integrity based on changes in trans-endothelial electrical resistance (TEER); in particular, we are interested in the virulence of a strain of *C. sakazakii* isolated from bovine feces;
2. Develop a site-specific mutagenesis procedure for *Cronobacter sakazakii* using a combination of cloning, random transposon insertion, and transformation.

LITERATURE REVIEW

Genus *Cronobacter*

Cronobacter spp. are Gram-negative, motile, facultative anaerobic rods of the family *Enterobacteriaceae* [1, 2, 28, 29]. They have been associated with necrotizing enterocolitis, sepsis, and meningitis in neonates and premature infants [1, 2, 28, 29]. On rare occasions, *Cronobacter spp.* associated diseases have also been reported in adults. The genus was first classified in the early 1960's as "yellow pigmented *Enterobacter cloacae"* due to its distinct yellow color on trypticase soy agar (TSA) and biochemical relatedness to the *Enterobacter* genus [2, 30]. However, it should be noted that not all *Cronobacter spp.* are able to produce the yellow color pigment [31, 32]. In 1980, "yellow pigmented *Enterobacter cloacae"* was re-classified into its own unique species of *Enterobacter sakazakii* due to further differences in genetic analyses and biochemical reactions from *Enterobacter cloacae* [2, 7].

In 2007, the entire *E. sakazakii* species was re-classified as the novel genus *Cronobacter* based upon polyphasic taxonomic analysis including 16S rRNA gene sequencing and DNA-DNA hybridization [1, 33]. The genus *Cronobacter* is currently divided into ten distinct species including *C. sakazakii, C. malonaticus, C. turicensis, C. muytjensii, C. dublinensis, C. universalis, C. condimenti, C.helveticus, C. pulveris,* and *C.zurichensis* [3, 4].

The natural reservoir of *Cronobacter* is unknown as species have been isolated from a wide range of sources. Species have been isolated from food products including cured meats, minced beef, sausage meat, raw cow milk, ultrahigh-temperature pasteurized cow milk, tofu, cereal products, rice seeds, lettuce, tomatoes, sour tea, sugar, and powdered infant formula (PIF) [12-14, 34]. Contaminated PIF has been implicated as the causative agent in the majority of neonatal or premature infant *Cronobacter* infections [6, 35]. It should be noted that PIF is not a

sterile product and can become contaminated any time during manufacturing or reconstitution. Species have also been isolated from household dust and from household and nursery utensils such as blenders and spoons [10, 13, 36, 37]. Kandhai et al. found that 30% of used household vacuum cleaner bags contained *Cronobacter spp.* (*n* = 16) while Breeuwer et al. reported 85% vacuum cleaner bags contained *Cronobacter spp.* (*n* = 7) [15, 38]. Species have also been isolated from clinical samples including the cerebrospinal fluid, urine, skin wounds, respiratory secretions, stomach aspirate, and anal swabs [5, 6, 39, 40]. In addition, *Cronobacter* spp. have been isolated from a number of environmental and animal sources such as soil sediments, water, crude oil, rats, Mexican fruit flies, rotting wood, bird feces, bison feces, and bovine feces [41-47]. Numerous studies have speculated that *Cronobacter's* ability to persist in a desiccated state and ability to form extracellular polymeric substances (EPS) may be an indication that their natural habitat is in the environment [16, 17]. In 2009, Schmid et al. proposed that plant roots in the soil may be *Cronobacter's* natural reservoir [16]. Their investigation found that *C. sakazakii, C. muytjensii, C. dublinensis, C. turicensis,* and *C. malonaticus* produce high levels of indole acetic acid (IAA), a plant hormone that stimulates plant growth through microbial colonization and root development [16].

Cronobacter spp. possess three known physiological traits that aid in environmental survival; a yellow pigment that protects the bacterium from ultra-violet (UV) light by absorbing photons, capsule and fimbriae that aid in adherence, and an increased ability to resist desiccation which contributes to increased survival in dry environments [32, 48]. The yellow pigmentation bestows a carotenogenic nature, which helps to stabilize cellular membranes and also influences membrane fluidity [32]. *Cronobacter spp.* are considered thermotolerant organisms that have been shown to survive in temperatures ranging from 5.5°C to 47°C [49, 50]. This indicates that

the bacteria are able to survive refrigeration temperatures, however a study performed by Iversen et al. found they are not able to replicate to reach numbers sufficient to cause disease at this low temperature [50]. Kandhai et al. found that *Cronobacter* is able grow at temperatures between 8° C and 47° C in sterile water, however their optimal growth temperature was found to range from 37° C to 43° C in PIF [49]. Kandhai also found that the genus has a relatively short lag time (1.7 hours) at this optimal temperature range [49]. Doubling times of this bacteria in rich media at 37°C was found to be around 20 minutes depending on the strain, which is similar to other genera in the family *Enterobacteriaceae* [51]. The incubation period of *Cronobacter spp.* in a human host remains unclear, as the moment of infection is often unknown due to numerous potential sources. In outbreaks where contaminated PIF was confirmed to be the causative agent illness began three to four days after initial ingestion [6, 9].

Several characteristic metabolic properties of the genus *Cronobacter* include the production of catalase and α-D-glucosidase, and the lack of the oxidase enzyme [13, 31, 52]. They have been found to be resistant to osmotic stress and dryness and have been recovered from desiccated infant formula after it had been stored for over 2.5 years [7, 53, 54]. It should be noted that the composition and low water activity (ca. 0.2) of the infant formula significantly attributes to bacterial survival [54-56]. In a comparison study by Breeuwer et al., it was found that *Cronobacter* may even be more suited to survive osmotic stress and drying than some *Escherichia, Salmonella,* and *Citrobacter* strains [54]. Breeuwer also observed that some *Cronobacter spp.* accumulate large amounts of mycose while in stationary phase which may play a role in protecting it from the effects of desiccation by helping stabilize the phospholipid membrane [15, 54, 57].

Diseases

Several species of *Cronobacter* are generally considered to be opportunistic pathogens known to infect neonates and premature infants. Although *Cronobacter* diseases are rare, they are often fatal. *Cronobacter* have been found to be the causative agent in a number of sporadic cases leading to necrotizing enterocolitis (NEC), septicemia, and meningitis [5, 6]. Mortality rates range between 40 – 80% for neonates and premature infants with survivors often suffering from long lasting or permanent mental or physical development delays [5, 58]. Diseases in adults caused by *Cronobacter spp.* are uncommon and have mostly been reported in individuals who are already immunocompromised [5, 58].

Necrotizing enterocolitis (NEC)

NEC is a gastrointestinal disease of the immature intestinal tract that causes portions of the bowel to undergo tissue death leading to its destruction. Signs include apnea, lethargy, vomiting, pneumatosis intestinalis, bradycardia, acidosis, septic shock, bloody stools, and anuria [59]. NEC has an incidence rate of between 2 to 5% in premature infants, but jumps to 13% in those weighing less than 3.3 pounds [6]. The mortality rate of NEC is between 10 – 55% in newborns [6]. Once a newborn has symptoms of NEC, the incurred inflammation and tissue death dramatically increases the ability of bacteria to transfer across the intestinal barrier into the blood stream. This translocation into the blood stream can easily lead to sepsis and even meningitis. The specific mechanism behind bacterial induced ischemic NEC is not fully understood, however inflammatory mediators such as platelet-activating factor (PAF) and tumor necrosis factor α (TNF-α) are suspected to play key roles [60]. The endotoxin of Gram negative bacteria has also been shown to lead to septic shock by triggering production of cytokines,

adhesion proteins and other enzymes that produce inflammatory mediators such as PAFs and TNF-α [60].

Meningitis

A systemic bacterial infection can contribute to further medical complications such as meningitis. Meningitis is characterized as the inflammation of the system of membranes surrounding the brain and spinal cord. These membranes are comprised of the dura mater, arachnoid, and pia mater, collectively known as the meninges. The reported rate of this disease is low, but the mortality rate among infants can be as high as 80% [7, 8]. The first association between *Cronobacter* and neonatal meningitis occurred in 1961, as reported by Urmenyi and Franklin [30]. Neonatal meningitis is often preceded by the development of sepsis which leads to the breaching of the BBB [61]. Ultimately, this results in inflammation of the ventricles of the brain (ventriculitis), formation of pus in the brain due to the inflammation from the infection (brain abscess), necrosis of the brain tissue due to the interruption of oxygen flow (infarction), and the accumulation of fluid in the brain (cyst formation) [5, 62]. In addition, about one-third of central nervous system diseases associated with *Cronobacter spp*. have been accompanied by seizures [63]. As mentioned, the prognosis for newborns with meningitis is often very poor and survivors often suffer from lifelong learning disorders, blindness, or deafness [64]. Studies by Stevens et al. and Harvey et al. have found that up to 74% of neonatal meningitis survivors suffer from adverse neurological conditions [64, 65].

Treatment

The standard treatment for individuals infected by *Cronobacter spp.* has been antibiotic therapy with a combination of gentamicin and trimethoprim-sulfamethoxazole [5, 66].

Unfortunately, emerging strains of *Cronobacter* have been found to be increasingly resistant to ampicillin, cefazolin, and penicillin, and so the use of the β-lactam antibiotic, cephalosporin, is often considered in a treatment regimen [5, 35]. Before administering antibiotics, antimicrobial susceptibility testing should be conducted to determine the most effective treatment plan. In cases of acute bacterial meningitis caused by *Cronobacter spp.*, a combination of gentamicin and ampicillin is considered the 'gold standard' according to Willis and Robinson and has been used successfully in a number of cases [67]. Gentamicin provides a broad-spectrum coverage against all Gram-negative bacilli and is rapidly bactericidal making it an effective choice [68]. One drawback of using gentamicin alone to treat meningitis is its inability to achieve adequate concentrations in the cerebral spinal fluid (CSF), hence the combination with ampicillin, which is able to translocate the BBB more easily [68]. Severe infections resulting in cerebritis, brain abscesses, or ventriculitis would require a longer therapy plan; however information is limited on an optimal duration. Treatment for newborn NEC includes providing bowel rests, gastric decompression, fluid repletion, starting parenteral nutrition feeding, and immediate antibiotic therapy [38]. Additionally, abdominal drains, colostomy, or emergency removal of the dead tissue may be necessary in more severe cases [38].

Prevention

The World Health Organization (WHO) and the American Academy of Pediatrics recommend exclusively breastfeeding newborns for the first six months of life [69]. A prevention method used to decrease the risk of newborn NEC is to provide hyperalimentation and oral feeds of human milk as early as possible [6, 21]. As the natural reservoir of *Cronobacter spp.* remains unknown, exclusively breastfeeding could protect the infant from a major confirmed source of infection, namely contaminated PIF. Educating health care providers and infant caregivers about

the potential dangers of contaminated PIF is also essential. This would likely result in decreased use of PIF and a stricter adherence to hygiene, cleaning, and disinfecting during reconstitution.

Outbreaks

Outbreaks associated with *Cronobacter spp.* are sporadic and the source of the infection is not always clear. Urmenyi and Franklin first reported the link between *Cronobacter spp.* and neonatal meningitis in 1961 after an outbreak in a nursery in England [30]. They reported on two infants that died in close time proximity of each other. Autopsy cultures of the infant's meninges, cerebral spinal fluid, and blood were found to contain *Cronobacter spp.* The source of the infection was never determined. The next major incidence of *Cronobacter spp.* infection occurred in 1983 in The Netherlands as reported by Muytjens et al. [70]. Muytjens investigated eight cases of neonatal meningitis and cerebritis. Five of the infected were from the same hospital and six of the eight died due to the incurred diseases. The two survivors later developed hydrocephalus and mental retardation. Environmental samples found that *Cronobacter spp.* were present in the prepared formula, and in the brushes and spoons used during reconstitution. The authors could not conclusively determine that the PIF was the cause of the outbreak, but this was the first report where *Cronobacter* contamination was associated with an outbreak. The first reported outbreak where PIF was confirmed as the source of *Cronobacter spp.* infection occurred in 1989 in the United States when four premature infants in the same intensive care unit experienced similar disease characteristics [9]. Sporadic newborn outbreaks of *Cronobacter spp.* infections cropped up during the early 2000's in numerous countries with the majority being confirmed nosocomial infections associated with contaminated PIF [6, 10, 11, 71-73] . The current neonatal infection rate in the United States is one *Cronobacter* infection per 100,000

infants and rises to 8.7 per 100,000 in low-birth weight neonates [74]. It is speculated that the incidence of infection may be under-reported in areas that lack appropriate medical microbiological facilities such as developing countries [29].

The first reported case of *Cronobacter spp.* that caused disease in an adult was in 1982 when a 76-year-old man, who had rectal adenocarcinoma and urinary retention, was diagnosis with *E. sakazakii* urosepsis [75]. In 1985, *E. sakazakii* was isolated from an adult's diabetic foot ulcer and in 1991 there was a report of a 75-year-old woman with *E. sakazakii* bacteremia [75, 76]. In 1996, Lai et al. reported on four adult hospital patients infected with *E. sakazakii* [77]. Two of the adults were initially suffering from pneumonia and the other two from elevated levels of bacteremia. Three of the four died due to complications, despite treatment. In 2001, a 26 year old woman in Budapest was diagnosed with vulvovaginitis due to an *E. sakazakii* infection [78]. It was believed that she was infected after bathing in a lake where *E. sakazakii* had been isolated. There are no reports of her having any sort of previous medical condition before the infection. In 2002, a multidrug resistant strain of *Cronobacter* was reported to have infected a surgical wound of a 64-year-old man with peripheral vascular disease [75]. The man was able to recover only after a partial leg amputation due to the infection. A review of case reports performed by Lai et al. in 2001 found that the majority of adults infected by *Cronobacter spp.* had serious underlying medical conditions [5].

In 2002, the International Commission for Microbiological Specifications for Foods classified *Cronobacter* as a severe risk for certain populations, specifically neonates and premature infants [38]. This was a large step in bringing the potential hazards of contaminated PIF to the health care provider's and the general public's attention. This move also helped motivate more research into the ecology, taxonomy, and pathology of *Cronobacter*. In 2004, the

Food and Agriculture Organization of the United Nations (FAO) and the WHO held a meeting regarding *Cronobacter* contamination in PIF that aimed to gather the information needed to revise the Recommended International Code of Hygienic Practice for Foods for Infants and Children [38]. This meeting led to changes in how PIF is processed during manufacturing and reconstitution that helps limit bacterial contamination overall.

Recently in 2011, Kimberly-Clark issued a product recall at the request of the Food and Drug Administration (FDA) of 1400 cases of their Kotex brand tampons whose ingredients were found to be contaminated by *Cronobacter sakazakii* [79]. The FDA released a statement that the use of the contaminated products could result in "vaginal infections, urinary tract infections, pelvic inflammatory disease or infections that can be life-threatening". Currently there have been over 150 reported cases of *Cronobacter*-associated infections all across the world ranging from all age groups [73].

Biofilms

Several species of *Cronobacter* have the ability to form biofilms [80, 81]. A biofilm is a sessile interface-associated consortium of bacteria that are tightly embedded in an endogenous slimy matrix called extracellular polymeric substance (EPS). The largest phenotypic difference between a biofilm and that of a planktonic life style is the increased resistance to environmental influences such as washing, abrasion, disinfectants, UV light, antibiotics, and heat seen in biofilms [82]. It should be emphasized that not all *Cronobacter* species are able to establish biofilms. Cruz et al. performed a biofilm capability study in *Cronobacter spp.* and found that only 26% of the strains they investigated (n = 43) were capable of forming biofilms [83]. Of the strains that Cruz investigated, including isolates of *C. sakazakii, C. malonaticus, C. dublinensis,*

C. muytjensii, and *C. turicensis*, the majority of biofilm forming isolates were from environmental sources.

Several *Cronobacter spp.* have been found to form biofilms on surfaces such as stainless steel, glass, polyvinyl chloride (PVC), silicone, polycarbonate, and enteral feeding tubes [17, 50, 81]. As mentioned, many of the newborn *Cronobacter* infections can be traced back to contaminated utensils used in the reconstitution of the PIF. The bacteria's ability to form biofilms on utensils can play a key role in their transmittance to humans. The pervasive nature and difficulty of removal makes biofilms a large concern for the food safety industry. Microbial biofilms can lead to significant economic losses as well as human lives.

Biofilm formation of *Cronobacter spp.* is highly dependent on temperature and nutrient availability. Kim et al. investigated the optimal temperature of *Cronobacter* biofilm formation and found that they attached to stainless steel material more proficiently at 25°C than at 12°C, with no biofilms being able to form at 12°C at all [81]. Iverson et al. discovered that *Cronobacter spp.* found in the reconstituted PIF itself were able to form biofilms on latex, silicon, polycarbonate, and stainless steel [50]. These types of materials are commonly used in infant feeding equipment and in utensils for reconstituting the PIF. Scheepe-Leberkühne and Wagner characterized the production of a highly viscous, anionic heteropolysaccharide capsular material of *Cronobacter spp.* which was speculated to enhance the adhesion and attachment to surfaces [84]. Lehner et al. evaluated 56 *C. sakazakii* strains for several features related to persistence and survival and found that some strains; express cellulose-like fibrils as an extracellular matrix component, adhere to hydrophobic and hydrophilic surfaces, produce EPS, produce cell-to-cell signaling molecules [17]. Lehner found that only 24.8% of their tested strains (n = 56) had the ability to produce EPS, which has been shown to play a key role in

biofilm formation and stabilization [17]. Lehner also found that *C. sakazakii* possess genes for cellulose biosynthesis. Cellulose biosynthesis plays a common role in structural formations by conferring mechanical, biological, and chemical protection and assists with formation of cell adhesion processes for infection [17]. The specific role of cellulose in *C. sakazakii* is still unknown, however Hartmann et al. discovered that cellulose did not contribute to adhesion to human epithelial colorectal adenocarcinoma (Caco-2) cells [80]. Hartmann used transposon mutagenesis and a flow cell system to investigate the genes that play a role in *C. sakazakii's* biofilm formation [80]. Their finding suggested that flagella and two yet-hypothetical proteins ESA_00281 and ESA_00282 contribute to adhesion onto Caco-2 cells [80]. More research is still needed to investigate the specific genes that play a role in biofilm formation.

Pathogenesis

There is an increasing library of knowledge regarding the pathogenesis of *Cronobacter spp.* at a molecular level. As mentioned earlier, the *Enterobacter sakazakii* species was reclassified in 2007 into the novel genus *Cronobacter* [1]. I will refer to any antiquated nomenclature as simply *Cronobacter spp.* for the purpose of this thesis. Pagotto et al. performed of the first studies into *Cronobacter spp.'s* virulence capabilities in 2003 by investigating the relationship between several putative virulence factors and the dose-response [19]. A suckling mouse model was used to discover that *Cronobacter spp.* produce an enterotoxin analogue [19]. The study went on to find that the intraperitoneal and oral minimal lethal doses for the mice were approximately 10^8 CFU/mouse [19]. An investigation performed by the World Health Organization (WHO) determined the approximate oral infectious dose for human neonates to be somewhere between 10^3 to 10^8 CFU [66].

In 2006, Mange et al. discovered that *Cronobacter spp.* was able to attach to intestinal and human brain microvascular endothelial cells (HBMEC) [21]. The use of their HBMEC model revealed two notable adhesion patterns; a diffuse adhesion and a formation of localized clusters on the cell surface [21]. Notably, when blood serum was added to bacterial growth media the *Cronobacter* isolates displayed the cluster adhesion pattern [21]. The specific mechanism by which this adhesion process occurs still remains to be determined; however several advances have been made. In 2008, Kim et al. performed a gentamicin protection model and confocal imaging of fluorescently tagged *Cronobacter spp.* to reveal the association between systemic infection and invasion of Caco-2 cells [85]. They found that entry into Caco-2 cells was enhanced in the presence of host cell actin filaments and microtubule structures. Kim also found that invasion was enhanced during disruption of the tight junctions between cell lines such as during an infection, which helps explain the opportunistic behavior of this organism.

In 2007, a study performed by Kothary et al. discovered a cell-bound zinc-containing metalloprotease (Zpx) that was unique to all of their 135 *Cronobacter spp.* isolates [27]. Zpx was shown to interact with the protease substrate azocasein, which led to rounding of Chinese hamster ovary (CHO) cells in tissue culture [27]. Kothary speculated that Zpx could play a key role in allowing *Cronobacter* to disrupt the cellular junctions of the GI tract or CNS leading to either NEC or meningitis, respectively. In 2008, Hunter et al. performed a study using an infant rat model that implicated over-expression of interleukin-6 (IL-6) and the Zpx protein to playing a key role in the pathogenicity of *Cronobacter spp.* associated NEC infection [86].

In 2008, Singamesetty et al. performed a study to investigate how *Cronobacter spp.* are able to invade HBMEC [22]. Singamesetty found that in order for this invasion to occur, it required the expression of the common Gram-negative protein, outer membrane protein A

(OmpA), to induce microtubule condensation [22]. OmpA has been found to play a key role in *E. coli* K1's invasion of HBMEC [23-25]. K1 has been implicated as the culprit in a number of neonatal meningitis incidences. A large amount of heat-stable endotoxin present in the PIF itself may also contribute to the ability of *Cronobacter spp.* to translocate across the BBB or lead to sepsis [18]. Giri et al. found that *Cronobacter spp.* were able to cross the tight monolayers of both Caco-2 and HBMEC in a transcytosis fashion [20]. Tight junctions (zonula occludens) of the BBB serve as a physical barrier that helps siphon molecular traffic into transcellular routes, meaning transfer through the cells themselves, as opposed to paracellular routes, meaning transfer through the intercellular spaces between the cells, in order to pass across the barrier [20, 87]. It was discovered by Townsend et al. in 2007 that *Cronobacter sakazakii* can survive within macrophages. The authors speculated that the ability to survive in macrophages may play a role in facilitating the crossing of the BBB by transferring across endothelial cells using a Trojan horse type mechanism [18].

The first partial *Cronobacter* genome was sequenced in 2001 [11]. But it was not until 2010, when Kucerova et al. sequenced the whole genome of *Cronobacter sakazakii* strain BAA-894, and in 2011 when Stephan et al. sequenced the genome of *Cronobacter turicensis* strain z3032, that major advancements in our understanding of virulence traits and genetic diversity took place [88, 89]. Sequencing revealed a 4.4 Mb chromosome and ~4392 genes, including 223 putative virulence genes such as the previously mentioned *ompA*, and a copper and silver resistance system (*cusC*) that had been linked to invasion of the BBB by strains of *E. coli* [88]. Additionally, it was found that several *Cronobacter sakazakii* strains contained two large plasmids (pESA3 and pCTU1) that harbor a number of putative virulence genes including iron acquisition systems, a *Cronobacter* plasminogen activator (*cpa*), and a Type 6 secretion system

[88, 90, 91]. In 2011, Franco et al. found that overexpression of the *cpa* gene in *E. coli* led to binding and cleavage of components of the complement cascade, namely C3, C3a, and C4b [91]. The complement system forms a transmembrane channel, called a membrane attack complex (MAC), on pathogenic bacteria that disrupts their phospholipid bilayer and effectively lyses them. The MAC is formed when small circulating proteins in the blood, such as C1, C3, C3a, and C4b, are recruited or created in a cascade fashion after stimulation by specific antigens. Franco went on to show that Cpa in *C. sakazakii* contributes to an increased survival rate in serum, illustrating that it could be a major virulence factor for the spread and invasion of this genus [91].

In 2011, Cruz et al. investigated the pathogenic mechanism of 19 *C. sakazakii* isolates, 6 *C. malonaticus* isolates, 13 *C. dublinensis* isolates, and 3 *C. muytjensii* isolates [83]. Cruz found that 86% of all the isolates tested were able to attach to HEp-2 cells and 35% of those attached were invasive. DNA sequencing and comparisons within the Virulence Factors Database (http://.www.mgc.ac.cn/VFs/) led Cruz to identify three putative virulence genes of note; a siderophore-interacting protein gene (*sip*), a type III hemolysin gene (*hly*), and the previously described *Cronobacter* plasminogen activator (*cpa*). Only 60% of their test isolates possessed the *sip* gene, 37% possessed the *hly* gene, and 28% possessed the *cpa* gene. This further illustrates the large diversity amongst the species of the genus *Cronobacter*.

The Blood Brain Barrier (BBB)

The BBB controls the movement of molecules between the blood in the body from the blood found in the CNS. It helps prevent harmful substances, such as pathogens or toxins, present in the bloodstream from gaining access to the brain. The BBB also controls the supply of essential nutrients into the CNS and mediates the removal of waste products. The barrier itself is

the result of the unique cellular interactions of the capillaries that permeate the brain and spinal cord. The cells of these capillaries and those neighboring them form tight, semi permeable junctions which is known as the BBB [92]. The basic cellular components are endothelial cells, astrocyte cells, and pericyte cells [92, 93]. These three cell lines work in concert with one another to form the tight junctions that make up the BBB. The endothelial cells create the capillaries themselves present in the brain and spinal cord while the astrocytes and pericytes help support and cover the gaps between them. The brain endothelial cells have both endothelial-like features, with a high activity of alkaline phosphatase and uptake acetylated low density lipoproteins, and epithelial-like features, with a low level of pinocytosis [87]. Astrocytes are the most numerous glial cells of the CNS. They coat the endothelial cells that form the capillaries present in both the brain and spinal cord. The astrocyte "end feet" are able to cover a large surface area and can easily encompass the spaces between endothelial cells to help enhance a tight physical cellular barrier [93, 94]. Astrocytes also play a key role in nutrient distribution to neurons, contribute to the maintenance of extracellular ion balance, and are an important source of regulatory factors like TGF-β and IL-6 [87, 95]. The third cell type, pericytes, cover approximately 22-32% of the endothelium and play a role in regulating endothelial proliferation, inflammatory processes, and angiogenesis [87, 96]. They are one of the least studied cellular components, however Armulik et al. found that permeability of the BBB increases in their absence [97]. Each cell type's involvement in the formation of the BBB is illustrated in Figure 1.

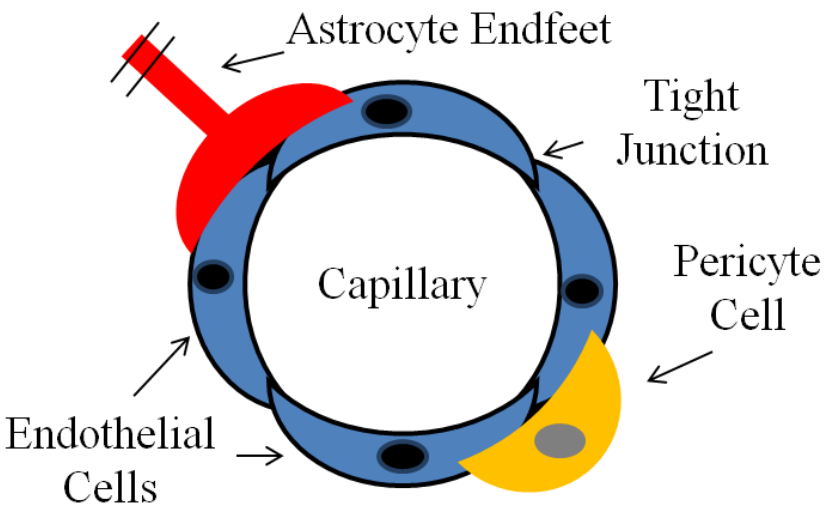

Figure 1. Cells involved in the blood brain barrier.

The BBB performs tasks such as leukocyte trafficking, osmoregulation, receptor-mediated signaling, and nutrient transport [98]. The transfer of compounds is tightly regulated and when intact, only small lipophilic molecules, hydrophilic molecules, and blood gases such as oxygen and carbon dioxide can freely diffuse across [87, 93]. Molecules such as glucose, nucleosides, and alkaloids are able to translocate the barrier by use of specific transport proteins while insulin and albumin are able to cross via receptor-mediated transcytosis and adsorptive transcytosis, respectively [95]. This strict regulation is important in maintaining a consistent microenvironment for neuronal signaling important for the CNS [95]. The most important function of the BBB is to protect the brain from the large fluctuations in ionic compositions that is experienced after eating a meal or exercising which would upset axonal and synaptic signaling [95]. The restriction of fluids and regulation of ionic movements between the blood and the brain helps create an interstitial fluid (ISF) medium that is optimal for neuronal function. This ISF is similar to blood plasma, but has a much lower protein content, a lower K^+ and Ca^{2+} content, and

higher Mg^{2+} levels [95]. The human BBB possesses several other unique properties specific to blood-barriers.

The permeability of the BBB is heavily dependent on the tight junctions between the endothelial cells that comprise the capillaries. The tight junctions primarily consist of three different integral membrane proteins that contribute to the flow of molecules through the barrier; occludin, claudin, and junction adhesion molecules (JAMs) [93]. These three protein types are anchored to the actin cytoskeleton of the endothelial cells by peripheral membrane proteins [21, 93]. Occludins are associated with the regulation of small hydrophilic molecular diffusion and the transmigration of neutrophils across the tight junctions [21]. Claudin proteins are one of the most important components of the BBB, they play a key role in the regulation of the paracellular barrier by controlling ion diffusion [21]. Abbott et al. discovered that the expression of claudin 3, claudin 5, and claudin 12 in the BBB contributes to lower permeability [95]. JAMs, specifically JAM-A, JAM-B, and JAM-C, are members of the immunoglobulin cell surface receptor subfamily [99]. They are localized between the endothelial cells and play a role in leukocyte transmigration and cell-to-cell adhesion throughout the barrier [99].

BBB models

The BBB can be a double edged sword in the sense that it functions to prevent pathogens from entering the CNS, but can also restricts the movement of therapeutics used to treat CNS disorders. This makes the BBB a large interest to pharmaceutical companies. An increasing scientific and therapeutic interest into the pathology and physiology of the BBB has led to the development of several *in vitro* models that are used as models. Such models are frequently used to investigate transportation and translocation of anticancer agents, immunosuppressive drugs, steroids, and cardiac drugs. *In vitro* models are the most feasible method for studying the BBB as

opposed to *in vivo* models in many cases. There have been a number of additional complications associated with studying the transport and metabolism using *in vivo* models of the BBB. These include the higher costs, increased labor, and the limited translational significance of animal models [87]. Additionally, i*n vivo* models are limited by the inaccessibility of the abluminal section of the brain capillary endothelial cells [87]. These *in vivo* issues helped push the development of several mono-culture, co-culture, and triple co-culture *in vitro* BBB models. *In vitro* models are highly repeatable, less expensive, less labor intensive, and are a reasonable representation of the real BBB [100].

Trans-endothelial electrical resistance (TEER)

TEER is the electrical resistance that is measured across cellular layers. TEER values are directly proportional to a cell barrier's confluency; the larger the TEER value the greater the cell integrity. The TEER measurements provide a reliable evaluation of the integrity of cellular barriers in both *in vivo* and *in vitro* models. TEER has been used in the past for a number of *in vitro* BBB models and is viewed as the standard to evaluate a cell barrier's integrity [101-111]. The first time TEER measurements were performed was in 1987 by Hart et al. and Rutten et al. [112, 113]. TEER measurements have traditionally been performed in *in vitro* models using an Epithelial Voltohmmeter (EVOM), an instrument specifically designed to perform TEER readings in tissue culture research (World Precision Instruments, United Kingdom). The EVOM is typically used in conjunction with either a STX2 style or endohm chamber style electrode to measure the cellular integrity of cells grown on microporous filter polyethylene terephthalate (PET) membranes. The potential advantages and drawbacks of both electrode types will be discussed below.

The handheld STX2 ‘chopstick’ style manual electrode has two unique prongs containing a silver/silver-chloride pellet that measures electrical voltage and a silver electrode to pass the current. To function properly, each prong is meant to be on either side of the PET membrane before electricity is passed through. Due to its size and material it is composed of, the STX2 style electrode can be quickly and easily sterilized with 70% ethanol. This style allows for a rapid TEER readings as well, with less potential for cross contamination [103]. One major drawback to using this style is that it can only provide a TEER reading at the specific point where the prongs are located at on the cellular barrier, and not an overall evaluation of the barrier as a whole. This can lead to less consistent TEER reading of the same PET membrane and as also between duplicates.

The stationary endohm chamber style electrode has a fixed electrode geometry that is able to measure the uniform density of a cellular barrier as a whole. This electrode style provides a more consistent and accurate TEER measurement with lower background interference. Unfortunately, this style is also more labor intensive to use and sterilize than the STX2 style electrode. The entire PET membrane needs to be removed from the cell culture plate and placed within the endohm chamber itself in order to measure the TEER. Due to the composition of the chamber, a longer sterilization procedure is required using a disinfectant specified by the manufacturer in place of 70% ethanol. World Precision Instruments, Inc. recommends using the EVOM in combination with the endohm chamber style reader for optimal accuracy; however the STX2 style still remains widely popular due to its simplicity. The TEER measurements are expressed as the resistance value (in Ohms) measured by the EVOM multiplied by the effective PET membrane area (the area that the cells are grown on) resulting in the Unit Area Resistance (UAR) in Ω x cm^2 [103].

Current Research

Site-specific mutagenesis

As mentioned, outbreaks of *Cronobacter* associated infections are rare and this has led to a shortage of research into their specific virulence genes. This has also resulted in the development of several less-than-ideal procedures for *Cronobacter* research. Current procedures used to create site-specific mutations in *Cronobacter spp.* tend to be expensive and labor intensive. Random mutagenesis procedures using transposon insertion kits has been used by Hartmann et al. and Johler et al. to generate large mutagenic libraries [32, 80]. They went on to use a combination of PCR, cloning, transformation, electroporation, and Southern blot analysis to identify specific sequences. However, these procedures were not designed to target specific gene locations and induce a mutation for further research. Franco et al. performed a successful site-specific mutation in the *cpa* gene by the use of mutagenic primers and suicide vectors to deliver a transposon to create an in-frame deletion [26]. These procedures are very time consuming and expensive. Characterizing large mutagenic libraries could take months to process, designing mutagenic primers can be complicated and time consuming, and purchasing suicide vectors and other reagents can be costly. Further research into the creation of a quicker and less expensive procedure to induce site-specific mutations in *Cronobacter spp.* is needed.

Investigation into *Cronobacter* pathogenesis

Cronobacter sakazakii has been reported to be capable of causing meningitis in neonates and premature infants. However, little is known about how this pathogenesis specifically takes place. With current mutagenesis procedures for *Cronobacter spp.* being very time consuming and expensive it would be wise to develop a simpler and less expensive method for research.

Ideally, this new method could be used to induce site-specific mutations in virulence genes believed to play a role in *C. sakazakii's* ability to breach the BBB and cause meningitis. These mutated *C. sakazakii* strains could then be challenged in an *in vitro* model of the BBB to evaluate the gene's effect on pathogenesis using TEER as an indicator.

In vitro co-culture model of the BBB

In vivo or *in vitro* models of the BBB can be used to investigate the pathogenesis of bacteria that are capable of causing meningitis. As described above, an *in vitro* model would be the most feasible choice as opposed to an *in vivo* model. Mono-cultures of the BBB using only endothelial cells may not accurately reflect the complex dynamics associated with the cell-to-cell interactions between the cell lines comprising the tight junctions. When designing a BBB model it would be prudent to incorporate more than one cell line in order to more closely mimic the real BBB. The roles of endothelial, astrocyte, and pericyte cells have been described above and an ideal *in vitro* model would incorporate them all. However, the use of three different cell lines in one model can become overwhelming and impractically time consuming for researchers. It is because of these issues that a co-culture model using endothelial cells and either astrocyte or pericyte cells would more accurately reflect the actual BBB and also limit the complexity to a practical and easily repeatable level.

METHODS

Table 1. Strains, plasmids, and phage used in methods

Name	ID	Source	Obtained from
11775	*Escherichia coli* K1	Clinical strain	American Type Culture Collections® (ATCC®) (Manassa, VA)
BAA-894	*Cronobacter sakazakii*	Clinical strain	ATCC® # BAA-894
C8-DIA	Astrocyte cells	*Mus musculus*	ATCC® # CRL-2544
CT2	*Cronobacter sakazakii*	Clinical strain	ATCC® #29544
DH5α	*Escherichia coli* K12	Lab-established strain	Invitrogen (Carlsbad, CA)
EOMA	Endothelial cells	*Mus musculus*	ATCC® # CRL-2586
EW-1	*C. sakazakii* CT2 with *zpx*::Tn5 and WT *zpx*	This study	This study
EW-A	*C. sakazakii* CT2 with *zpx*::Tn5	This study	This study
HV-1	*E. coli* DH5α with *zpx*::Tn5	This study	This study
N72	*Cronobacter spp.*	Bovine feces	North Dakota Veterinary Diagnostic Lab Bovine Fecal Sample, Fargo, ND
pCRE1	P1 Bacteriophage	Maruyama et al. [114]	ATCC® #77368
p*Zpx*	pGEM plasmid with inserted *zpx*	This study	This study
zpx::Tn5	*zpx* with inserted Tn5 transposon	This study	This study

Co-Culture Blood Brain Barrier Model

Eukaryotic cell propagation and seeding

Secondary mouse astrocyte cells (C8-DIA) and endothelial cells (EOMA) (Table 1) were propagated in 75 cm^2 polystyrene cell culture flasks (Sigma-Aldrich, St. Louis, MO) in Dulbecco's Modified Eagle Medium (DMEM) (Corning cellgro, Manassas, VA) supplemented with 1.5 g/L sodium bicarbonate and 10% fetal bovine serum (complete DMEM) (Atlanta Biological, Lawrenceville, GA). The media used to maintain the cell lines was also supplemented with penicillin and streptomycin at concentrations of 200 µg/mL (Corning cellgro, Manassas, VA). Cells were incubated in a Sanyo™ professional cell culture CO_2 incubator with inCu-saFe™ and SafeCell™ UV integrated contamination control technology (Thermo Fisher Scientific, Waltham, MA) at 37° C with 5% CO_2 concentration. Cells were passed once a week by treatment with 0.25% trypsin (Corning cellgro). C8-DIA cells ($6.4x10^3$) were seeded onto the basal side (Figure 2) of upturned 0.4 µm polyethylene terephthalate (PET) cell culture inserts (BD, Franklin Lakes, NJ) and incubated at 37° C 5% CO_2 for four hours to facilitate attachment. The PET inserts were inverted to their manufacturer's defined orientation and the C8-DIA cells were incubated in complete DMEM without antibiotics for six days with media replacement every 48 hours. EOMA cells ($2.0x10^4$) were seeded onto the apical side (Figure 2) of the PET inserts six days after the C8-DIA cells were seeded. Cell culture inserts were incubated for an additional six days with media replacement every 48 hours.

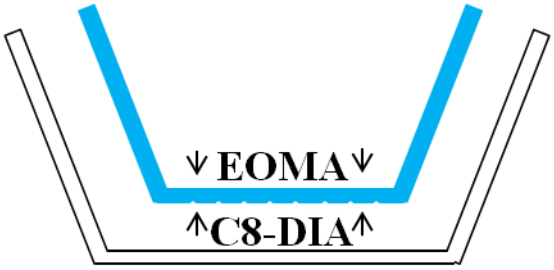

Figure 2. BBB co-culture model schematic. The EOMA cells were seeded onto the apical side of the PET cell culture inserts while the C8-DIA cells were seeded on the basal side.

Bacterial propagation and infection procedure

E. coli strain K1 (ATCC 11775) and *E. coli* strain DH5α (Table 1) were selected as positive and negative controls, respectively. The *C. sakazakii* clinical strain BAA-894 [88] and bovine fecal strain N72 [47] were selected as experiment strains for this study. An isolated colony of each treatment was transferred to Luria Bertani (LB) broth (EMD Chemicals, Gobbstown, NJ) and incubated at 37° C, shaking at 200 rpm, overnight. Treatments were adjusted to a final concentration of 1000 CFU/mL. Each bacterial culture was inoculated onto the apical side of each PET insert that was previously seeded with EOMA cells (Figure 2). Bacteria cultures were inoculated in quadruplicate with cellular and blanks controls both in duplicate in a 24 well cell culture plate (Figure 3). Culture plates were incubated at 37° C in 5% CO_2.

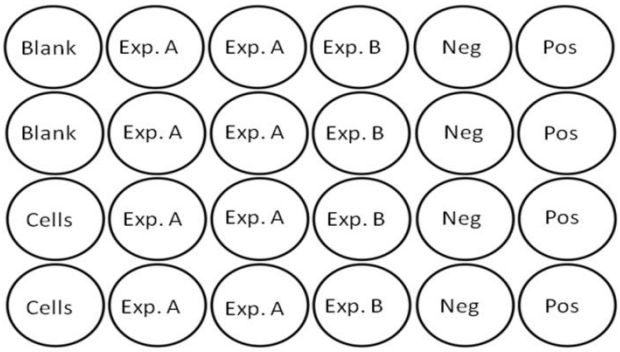

Figure 3. Plate set-up for the BBB co-culture. A single media blank (Blank) was performed in each 24 plate along with cell controls (Cells) performed in duplicate. Negative (Neg) and Positive (Pos) controls were performed in quadruplicate and experimental strains (Exp. A and Exp. B) were performed in either quadruplicate or repeated eight times.

Trans-endothelial electrical resistance (TEER) readings

The electrical resistances of the co-culture cellular barriers were measured using an epithelial voltohmmeter (EVOM) (World Precision Instruments, Hertfordshire, UK) in conjunction with the stationary electrode chamber, ENDOHM-6 (World Precision Instruments). The ENDOHM-6 is designed to measure 6.0 millimeter sized tissue culture cups that are used in 24 well plates. Each instrument was used according to the manufacturer's instructions with three important side notes;

1. The PET inserts were washed with PBS before addition of the reading media (DMEM) in order to remove any residual culture media,
2. The culture media on the apical side of the PET inserts was preserved during the reading process, stored at 37° 5% CO_2 during TEER reading, and reapplied after,
3. The ENDOHM - 6 was soaked in Sporicidin® disinfectant (Contec, Spartanburg, SC) for 30 minutes and rinsed with PBS between TEER readings of different treatment groups.

During the TEER reading process, the cell culture inserts were removed from the 37°C 5% CO_2 incubator and returned after the readings were complete. Each experimental TEER value at 24 hours was subtracted from the TEER value of the PET insert without cells (media blank), resulting in the 'True Tissue Resistance'. This True Tissue Resistance (Ω) value was then multiplied by the effective membrane area of the PET insert (0.4 cm^2 for the inserts used in this case); resulting in the Unit Area Resistance (UAR) (Ω x cm^2). TEER was measured for each treatment at hour 0 (before addition of bacteria) and after 24 hours of bacterial exposure.

Statistical analysis

The UAR was converted to percent change over time from hour 0 to 24 for each experimental PET insert culture and control using the blank media control UAR value as a base. The UAR was analyzed using SAS 9.2 program. A general linear model (GLM) was used and a Duncan's multiple range test was performed to compare the significance between hour 0 and 24. The parameters for the GLM are listed in Table 13 in the Appendix section and the Duncan's multiple range test parameters is listed in Table 4.

Site-Specific Mutagenesis Procedure

Table 2. Primers used in the site-specific mutagenesis procedure.

Primer	Primer Sequence	Annealing Temperature	Target	Source
Esak 5P (Forward)	5'-AACCAGTCACGTTATCCAACC-3'	62.5° C	*zpx*	Kothary et al. [27]
ES-R2 (Reverse)	5'-TCACAACACCCCTGTGGTT-3'	64.1° C	*zpx*	Kothary et al. [27]
TnKanF (Forward)	5'-GCCCGATGCGCCAGAGTTGT-3'	73.0° C	EZ-Tn5™ <KAN-2> Transposon	EZ-Tn5™ <KAN-2> Insertion Kit (EPICENTRE, Madison, WI)
TnKanR (Reverse)	5'-CGACTCTAGAGGATCCCCGCC-3'	69.0° C	EZ-Tn5™ <KAN-2> Transposon	EZ-Tn5™ <KAN-2> Insertion Kit (EPICENTRE, Madison, WI)

Isolation of putative virulence gene *zpx*

To prepare DNA lysate, *C. sakazakii* CT2 isolates were struck onto Luria Bertani (LB) agar (EMD Chemicals, Gobbstown, NJ) and incubated at 37°C overnight. An isolated colony was inoculated into 40 µl of TE (10 mM Tris-HCl, 1 mM EDTA, pH 8.0) containing 1% Proteinase K (AMRESCO, Solon, OH). The mixture was incubated in a thermocycler (MJ Research, Ramsey, MN) for 10 minutes at 55°C followed by 10 minutes at 80°C. The DNA lysate was adjusted to a final volume of 120 µl in ddH_2O and centrifuged at 6000 rpm for 5 minutes.

Amplification of the *zpx* gene (1026 bp) was performed by using primers Esak 5P and ES-R2 (Table 2) [27]. PCR reactions were created using 2.0 µL of the prepared CT2 genomic DNA, 17.875 µL ddH_2O, 0.25 µL Esak 5P, 0.25 µL ES-R2, 0.5 µL dNTPs, 5.0 µL 5x buffer, and 0.125 µL taq polymerase. The PCR reactions were incubated in a thermocycler for an initial denaturation at 95° C for 60 seconds, 25 cycles of 94° C for 30 seconds, 62° C for 20 seconds, 72° C for 30 seconds, and a final elongation at 72°C for 5 minutes. Amplicons were visualized by gel electrophoresis using 1.0% agarose, EZ Vision® loading dye (AMRESCO, Solon, OH), and fluorescent light.

Cloning into pGEM

Cloning of the *zpx* amplicon into a pGEM®-T Easy Vector (Promega, Madison, WI) was performed according to the manufacturer's instructions. Briefly, the pGEM vector's multiple cloning sites allow for ligation of PCR products into the plasmid after restriction enzyme digestion using EcoRI (Promega, Madison, WI). Successful insertion of a PCR amplicon interrupts the vector's *lacZ* gene, enabling selection of white colonies on Xgal (5-bromo-4chloro-3-indolyl-β-D-galactopyranoside).

Chemically competent cells and transformation

The plasmid DNA was transformed into chemically competent *E. coli* DH5α (Table 1). DH5α was made chemically competent by inoculating a single colony into 100 mL of LB broth and incubating at 37°C, while shaking at 200 rpm for 4 hours. A 50 mL portion of the broth culture was incubated on ice for 10 minutes followed by centrifugation at 4100 rpm for 10 minutes at 4° C. The supernatant was removed and the remaining 50 mL of broth culture was added, incubated on ice for 10 minutes, and centrifuged again. The supernatant was removed and

the pellet was re-suspended in 30 mL of ice-cold $MgCl_2$: $CaCl_2$ (80mM: 20mM). The mixture was centrifuged, the supernatant discarded, and the pellet re-suspended in 4 mL of ice-cold 0.1 M $CaCl_2$. In order to prepare the cells for freezing, 70 µL of DMSO was added, incubated on ice for 15 minutes, and an additional 70 µL of DMSO was added. Cells were snap-frozen in liquid nitrogen and stored at -80°C.

For the transformation, 25 ng of plasmid DNA was combined with $4.0x10^7$ of chemically competent DH5α cells. 25 ng of pUC18 DNA and ddH_2O was used as positive and negative controls, respectively. Mixtures were incubated on ice for 30 minutes, heat shocked at 42°C for 90 seconds and immediately placed in an ice bath for 2 minutes. 800 µL of super optimal broth (SOC) media (2% tryptone, 0.5% yeast extract, 8.6 mM NaCl, 2.5 mM KCl, 20 mM $MgSO_4$, 20 mM glucose) was added and incubated an additional 45 minutes at 37°C. Experimental samples and controls were plated onto Xgal agar containing ampicillin (amp) (50 µg/ mL). Following a 37° C overnight incubation, white colonies were screened for the presence of *zpx* via PCR and gel electrophoresis. Plasmid preps were performed using a Quick Lyse Miniprep Kit (QIAGEN, Germantown, MD) per the manufacturer's instructions. The isolated plasmid was digested using *Eco*RI (Promega, Madison, WI) to extract the inserted sequence. Digests were performed by combining 1.0 µg of the plasmid DNA, 2.5 µL of 10X multicore buffer, 12 units of *Eco*RI, and 9.5 µL of ddH_2O. The mixture was incubated at 37°C for 4 hours and visualized by gel electrophoresis. The resulting plasmid was named p*Zpx* (Table 1).

Transposon insertion into p*Zpx* and transformation

An EZ-Tn5™ <KAN-2> Insertion Kit (EPICENTRE, Madison, WI) was used to randomly insert a Tn5 transposon (1221 bp) containing a non-functional transposase gene and a

kanamycin resistance marker gene into the p*Zpx*. The kit was used according to the manufacturer's description.

The Tn5 reaction mixture was transformed into One Shot® Top10 Chemically Competent *E. coli* (Invitrogen, Grand Island, NY) according to the manufacturer's instructions. Thirty white colonies (Tf 1 – 30) on Xgal containing kanamycin (kan) (50 µg/ mL) /amp (50 µg/ mL) were selected. Each colony was inoculated into LB kan/amp (50 µg/ mL) broth for further *zpx* characterization. The genomic DNA of each culture was isolated and *zpx* gene amplified by PCR and visualized by gel electrophoresis. HV-1 (Table 1) was found to have an amplified *zpx* band size of about 2247 bp (Figure 8), indicating successful interruption of the *zpx* gene with the Tn5 transposon. The HV-1 *zpx* amplicons were digested using *Eco*RI and visualized by gel electrophoresis. The amplicon digest produced two bands that were approximately 1026 bp (wild type *zpx*) and 1221 bp (Tn5KAN) in sizes. The *zpx* gene of HV-1 was termed *zpx*::Tn5 (Table 1).

Infection with pCRE1 bacteriophage

HV-1 was infected with pCRE1 bacteriophage (Table 1). A colony of HV-1 was inoculated into 5 mL of LB kan /amp (50 µg/ mL) broth and incubated at 37°C while shaking at 200 rpm overnight. 50 µL portion of the overnight culture was inoculated into 5 mL of LB broth/0.2% glucose/5 mM $CaCl_2$ and incubated at 37°C while shaking at 200 rpm for one hour. After incubation, 100 µL of pCRE1 bacteriophage was added into a flask protected from light and incubated at 37°C while shaking at 200 rpm for 3 hours. To lyse any remaining cells, a volume of 100 µL of chloroform was added and centrifuged at 8700 rpm for 10 minutes at room temperature. The supernatant was carefully removed and transferred to a new flask where an additional 100 µL of chloroform was added. The phage lysate was stored at 4°C until use.

Transformation

The phage lysate was transformed into chemically competent *C. sakazakii* CT2 cells (Table 1). A phage lysate volume of 100 µL was added to $4.0x10^7$ competent CT2 cells and 25 ng of pUC18 DNA and ddH_2O was added to competent cells to serve as positive and negative controls, respectively. Competent CT2 cells infected with the phage lysate and the positive and negative controls were incubated on ice for 30 minutes and heat shocked in a 42°C water bath for 90 seconds. Following a 2 minute ice bath incubation, 800 µL of SOC media was added, and incubated at 37°C for 45 minutes. 200 µL of the experimental phage culture was plated onto LB kan (50 µg/ mL). The positive control was plated onto LB amp (100 µg/ mL) and the negative control was plated onto both LB kan and LB amp. Plates were incubated at 37° C overnight and the resulting strains from the experimental phage cultures were named EW-1 (Table 1).

Characterizing EW-1 mutants

A colony of EW-1was converted to DNA lysate and used in several PCR reactions in order to further characterize the mutation. PCR reactions were performed using the forward *zpx* gene primer and the reverse of the transposon primer (Table 2) and vise versa. The primer grouping PCR reactions were incubated in a thermocycler for an initial denaturation at 95° C for 60 seconds, 25 cycles of 94° C for 30 seconds, 62° C for 20 seconds, 72° C for 30 seconds, and a final elongation at 72°C for 5 minutes. Amplicons from these primer groupings were visualized via gel electrophoresis (Figure 7). A PCR reaction to amplify the *zpx* gene of EW-1 was performed and visualized via gel electrophoresis (Figure 8). Plasmid preps were performed using a Quick Lyse Miniprep Kit (QIAGEN, Germantown, MD) and visualized by gel electrophoresis (Figure 9).

Linear transformation by electroporation

The *zpx*::Tn5 gene was amplified from HV-1 via PCR and transformed into competent CT2 cells by electroporation. Electrocompetent CT2 cells were created by inoculating 25 mL of an overnight CT2 broth culture into 500 mL of LB broth and incubating at 37° C while shaking at 250 rpm. Optical density at a wavelength of 600 nm was measured every 20 minutes in order to achieve an OD_{600} of 0.4 followed by an ice bath for 30 minutes. The culture was centrifuged at 1400 rpm for 15 minutes at 4° C. The supernatant was decanted and the pellet re-suspended in ice-cold ddH_2O. The culture was centrifuged at 1400 rpm for 20 minutes at 4° C, supernatant discarded, and pellet resuspended in 200 mL of 10% glycerol. The glycerol wash step was repeated once again followed by a final centrifugation under the same parameter and the supernatant was decanted. The pellet was re-suspended in 1.0 mL GYT (10% glycerol, 0.125% yeast extract, 0.25% tryptone) and diluted 1:100. $4.0x10^7$ electrocompetent CT2 cells were incubated on ice for 10 minutes and 5 µL of the purified *zpx*::Tn5 DNA was inoculated. 10 µL of pUC18 DNA (10 ng/µL) and ddH_2O served as positive and negative controls, respectively. The cultures were transferred to chilled 0.1 cm electroporation cuvettes (Bio-Rad, Hercules, CA) and were incubated on ice for 10 minutes before being transferred to the electroporation apparatus (Bio-Rad, Hercules, CA). Cuvettes were electroporated at T= 2.5 kV, V= 1.66 kV parameters, after-which 1.0 mL of SOC media was added and incubated at 37°C for 1 hour. The experimental culture was plated onto LB kan (50 µg/mL), the positive control was plated onto LB amp (50 µg/mL), and the negative control was plated onto both LB kan and LB amp. Plates were incubated at 37°C overnight. The resulting experimental strains were named EW-A (Table 1).

Characterizing EW-A mutants

A colony of EW-A was converted into genomic DNA, used in a PCR reaction to amplify the *zpx* gene, and visualized via gel electrophoresis (Figure 8). PCR reactions were performed using the forward *zpx* gene primer and the reverse of the transposon primer (Table 2) and vise versa. Additionally, plasmid preps were performed using a Quick Lyse Miniprep Kit (QIAGEN, Germantown, MD) and visualized by gel electrophoresis (Figure 9).

RESULTS AND DISCUSSION

This study utilizes a co-culture *in vitro* model of the BBB using murine astrocyte and endothelial cells based on a previously established assay for the investigation of *Cronobacter sakazakii* pathogenesis [47, 115]. Current methods that have been used successfully to induce mutations in genes of *C. sakazakii* include the use of mutagenic primers, transposons, and suicide vectors [26, 27, 32, 80]. This study also proposes a novel site-specific mutagenesis procedure that is both rapid and cost effective. This procedure involves using a combination of cloning, random transposon insertion, PCR amplification, and transformation of a linear DNA product. A second procedure was developed using a combination of transduction and transformation, but was unable to successfully replace the wild type gene. As specific pathogenesis mechanisms of *C. sakazakii* remain largely unknown, this co-culture model and mutagenesis procedure will be used in future studies to investigate the pathogenesis of these organisms.

Co-Culture Blood Brain Barrier Model

The primary purpose of this study was to establish a consistent and accurate *in vitro* representation of the human BBB to be used to investigate *C. sakazakii* pathogenesis. The main cellular components of the BBB are discussed in detail in the Blood Brain Barrier (BBB) section of the Literature Review. A major contributing factor that led to our justification of a cellular co-culture model of over a mono-culture model of the BBB was a comparative study performed by Koval et al. in 2010 [47]. Koval found that a co-culture model of endothelial and astrocyte cells provided greater TEER values overall when compared to a mono-culture model with endothelial

cells alone. This was likely due to the addition of the astrocyte cells, whose end feet reinforce the tight barriers between the endothelial cells leading to increased barrier integrity.

The co-culture model developed in this study was a modification of a previously established model created by Gaillard et al. in 2001 [115]. Gaillard created a flexible and reproducible co-culture model of the BBB using bovine brain capillary endothelial cells (BCEC) and rat astrocyte cells on polycarbonate semi-permeable filter inserts. Gaillard's research pioneered the establishment of a functional, flexible, and reproducible co-culture model of the BBB using endothelial and astrocyte cells. Much of our basic eukaryotic co-culture model set-up closely mimicked theirs. However, Gaillard did not use their model to investigate bacterial pathogenesis, instead they characterized the cells based on several specific BBB properties including; expression of specific cell markers, restriction of paracellular transport, and the tight junction formation between the cell lines using TEER. Another major difference in procedures; they used the STX2 "chopstick" style electrode to determine the cellular resistance while this study used the endohm chamber electrode.

This study utilized the EVOM in combination with the endohm chamber reader as opposed to the hand-held STX2 electrode based on a pilot comparison experiment of both. Preliminary studies using the STX2 electrode confirmed the drawbacks as discussed in the Trans-endothelial Electrical Resistance (TEER) section of the Literature Review. The mobility and small electrode size of the STX2 could only provide UAR at that specific point on the PET cell culture insert. This led to dramatically varied TEER readings, which was anywhere from 100 Ω to 300 Ω, on the same PET cell culture insert depending on the electrode's placement. Switching to the endohm chamber remedied this issue as it provided a consistent UAR reading over the entire PET cell culture insert.

Two *C. sakazakii* strains were selected for use in the co-culture model of this study, N72 and BAA-894. *C. sakazakii* N72 was isolated from bovine feces in a lab at North Dakota State University and its pathogenicity remains unknown. The *C. sakazakii* BAA-894 strain has had its entire genome sequenced in 2010 and was postulated to be non-pathogenic based on identification of known virulence factors [88]. This study used two *E. coli* strains to serve as negative and positive controls. The nonpathogenic *E. coli* K12 strain, DH5α, was used as the negative control. DH5α is a lab-attenuated strain that has never been reported as the causative agent in a meningitis case. This made it an ideal choice as the negative control for our assay. *E. coli* strain K1 was used in this study as a positive control due to its pathogenic nature and ability to disrupt the BBB leading to meningitis. The results indicated that the controls functioned as expected, with the negative control having significantly less decrease in UAR over the course of time compared to the positive control, which lost significant barrier resistance over 24 hours. A high UAR value indicates a greater cell barrier integrity and vise versa.

TEER readings using the endohm chamber electrode went smoothly and without complication, with a few exceptions. TEER readings tended to be lower for treatments located on the edges of the 24 well plates as opposed to those located in the center of the plate. Additionally, there were several anomalous readings in Plate 4 A (Table A6). Noticeably lower TEER readings were observed in several treatments of that plate. These TEER values were observably lower than duplicates of the same treatments in other plates. The trend continued in each treatment where they were observed and continued to the hour 24 reading. These inconsistencies were resolved by calculating the percent change from hour 0 to 24 for each raw TEER value. The raw TEER data used to calculate the percent change is listed in Tables A1–A5.

Each experimental treatment and control was repeated 20 times across ten co-culture plates. A sample of the collected raw TEER data is below in Table 3. A general decrease in UAR values can be observed in all treatments over the time frame of this study. As seen, the cell control's UAR remains relatively the same over the course of 24 hours. In general, the experimental strain, N72, has about a 20 UAR decrease over the course of 24 hours, however the experimental strain, BAA-894, has a negligible decrease over the same time. The negative control also has a negligible decrease in UAR, whereas the positive control has about a 20 UAR decrease. The raw UAR data tables can be directly correlated to the co-culture plate set-up in Figure 3 and Figure 4. Table 3 below is just one example of the collected UAR data; the complete UAR data is located in Tables A1–A5 of the Appendix section.

Table 3. Example of collected raw TEER data.

Plate 3 A
Unit Area Resistance (UAR) ($\Omega * cm^2$)

Time						
0hr	Blank	N72	N72	BAA-894	Negative	Positive
	65.7	130.8	129.6	138.6	131.4	125.7
	Cells	143.7	126.6	132.9	129.3	118.8
	122.7	120	123.3	115.5	125.4	134.7
	138.3	127.2	127.8	132.9	131.4	120
24hr	Blank	N72	N72	BAA-894	Negative	Positive
	56.7	120.3	101.4	133.2	131.7	109.8
	Cells	124.5	103.8	126.6	134.7	101.7
	127.2	98.4	100.2	110.1	115.8	106.8
	120.6	110.4	110.1	133.5	112.5	108.6

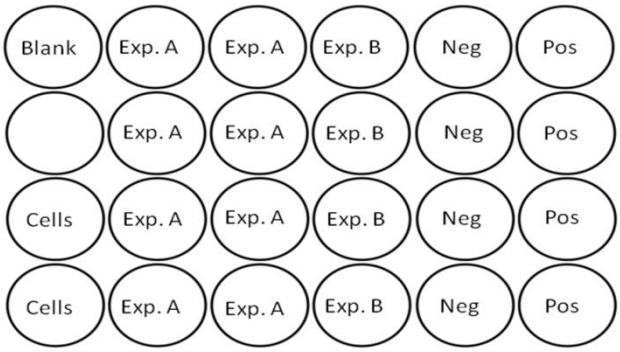

Figure 4. Co-culture plate set-up.

The calculated percent change TEER data for each treatment is listed in the Appendix section (Table 12). As discussed earlier, percent change was calculated from hour 0 to 24. The lower the percent change from hour 0 to 24 indicates a smaller change in barrier integrity over the course of 24 hours. A larger the percent change from hour 0 to 24 indicates a large change in barrier integrity over the course of 24 hours. The percentage of remaining barrier integrity for each treatment group is displayed in Figure 5 below. This figure illustrates how much of the cellular barrier was left intact after a 24 hours exposure to each treatment. As each treatment (n = 20) was transformed into the percent change over 24 hours there are no standard deviations available for this incarnation. The barrier that was most intact after 24 hours was from the Negative *E. coli* DH5α control, as was expected. Integrity proceeded to decrease across the other treatment groups from BAA-894, N72, and the Positive *E. coli* K1 control, in that order. The cellular barrier was least intact after 24 hours in the Positive control, which was also expected.

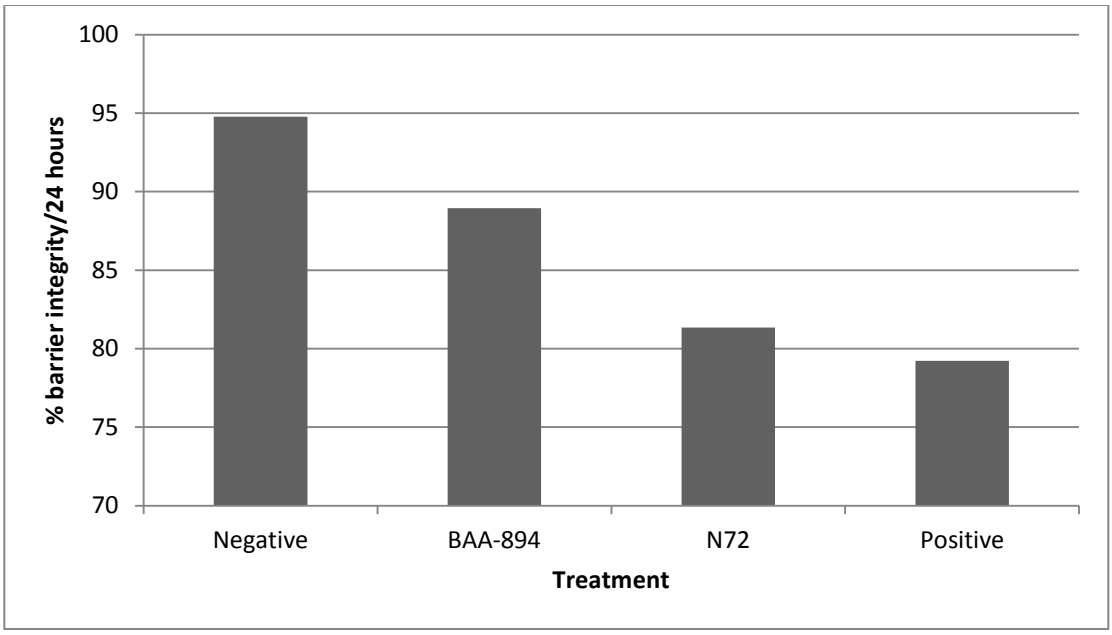

Figure 5. Remaining barrier integrity over 24 hours. Illustrates the percentage of the cellular barrier that remained for each treatment over the course of 24 hours.

The Duncan Groupings calculated from the percent change from hour 0 to 24 is displayed in Table 4. The model parameters are listed in the Appendix section. The negative control and BAA-894 were grouped together, indicating no significant difference (α=0.05). The positive control and N72 were also grouped together, indicating that there was no significant difference between the two strains. The negative control and BAA-894 were found to be significantly different from the positive control and N72. The fit diagnostics, distribution data, residuals, and GLM parameters for each control and experimental treatments are listed in the Appendix section (Figures A1 – A4).

Table 4. Duncan's multiple range test parameters and groupings. This test controls the Type I comparison-wise error rate, not the experiment-wise error rate.

Alpha	0.05
Error Degrees of Freedom	76
Error Mean Square	0.012971

Means with the same letter are not significantly different.			
Duncan Grouping	**Mean**	**N**	**Treatment**
A	0.94779	20	Negative
A			
A	0.88943	20	BAA-894
B	0.81334	20	N72
B			
B	0.79217	20	Positive

Number of Means	**2**	**3**	**4**
Critical Range	0.07173	0.07547	0.07795

Several assumptions can be made based on the Duncan Multiple Range Test groupings. As mentioned, the negative control and BAA-894 were classified together into the same grouping while the positive control and N72 were grouped together in another. This means that the negative and positive controls were not grouped together, signifying that they are significantly different from one another and have different effects on the co-culture model. This means that the co-culture BBB model functioned appropriately and can be used as a feasible model to investigate bacterial pathogenesis with the use of these controls in the future. The

Duncan Groupings of *C. sakazakii* strain BAA-894 with the negative control was another result worthy of note. This agrees with the genomic comparison performed by Kucerova et al. which found that BAA-894 had decreased virulence properties compared to other *C. sakazakii* strains isolated from the meninges of newborns with meningitis [88]. So, it is not surprising that the Duncan Grouping results grouped BAA-894 together with the K12 *E. coli* negative control strain, which is also considered to be non-pathogenic.

More interesting was the grouping of the experimental *C. sakazakii* N72 strain with the K1 *E. coli* positive control. *C. sakazakii* N72 was isolated from the feces of a healthy bovine in a laboratory at North Dakota State University. This is the only known *Cronobacter spp.* to be isolated from the feces of bovine cattle. This discovery may indicate that *Cronobacter spp.* is a commensal bacterium of the intestinal tract of that animal. That the results indicated that N72 was in the same category as our pathogenic positive control is concerning. This could be an indication that N72 is a pathogenic strain of *C. sakazakii*. As discussed earlier, *Cronobacter spp.* have been shown to display increased resistance to heat and the effects of pasteurization [12]. It is possible that N72 present in the bovine's feces could contaminate milk during the harvesting process. If raw milk was contaminated with N72, it may survive the pasteurization process. *Cronobacter spp.* have also been shown to be able to form biofilms on stainless steel surfaces [81]. The dairy industry commonly stores milk in large stainless steel vats. Should a biofilm of N72 form inside one of these vats, it would lead to contamination of any milk stored in that container. This would also lead to further contamination of other food products that incorporate milk as an ingredient. As mentioned previously, the majority of *Cronobacter*-associated infections in newborns can be traced back to contaminated PIF. This contamination could have been the result of contact with a biofilm of *Cronobacter* sometime during processing or

reconstitution. The ability of N72 to resist heat treatments such as pasteurization and its ability to form biofilms has yet to be investigated. The potential pathogenic nature of N72 makes it of interest for further characterization.

Site-Specific Mutagenesis Procedure

The second study involved the development of a simple, rapid, and cost effective procedure to induce site-specific mutations in putative virulence genes of *C. sakazakii*. Current methods to induce site-specific mutations in *Cronobacter spp.* involve screening large mutagenic libraries, creating mutagenic primers, and the use of suicide vectors [27, 32, 80]. We set out to create a more straightforward, less time consuming, and cost effective procedure to induce a mutation in the *zpx* gene of *C. sakazakii.* The *zpx* gene was previously characterized and described in detail by Kothary et al. in 2007 [27]. This gene codes for a protease enzyme and was present in all of the 135 *Cronobacter spp.* that Kothary examined. The gene was found to be responsible for rounding of Chinese hamster ovary (CHO) cells in tissue culture. Based on their research, Kothary speculated that the *zpx* gene product could play a key role in the ability of *C. sakazakii* to breach cellular barriers, specifically the blood brain barrier or the cellular barrier of the intestinal tract.

PCR amplification of the *zpx* gene of the wild type *C. sakazakii* strain CT2 resulted in a single band near the 1000 bp marker (Figure 8). Kothary et al. determined that the *zpx* gene has a size of 1026 bp and the band size after amplification of the wild type CT2 indicates that it possesses the wild type *zpx* gene. The *zpx* amplification of HV-1 resulted in a single band between 2000 and 3000 bp (Figure 8). HV-1 was the *E. coli* strain containing *Zpx*::Tn5. The transposon used for insertion was 1221 bp in size, and insertion of this transposon into the wild

type *zpx* gene the amplification would have resulted in a 2247 bp band size, or a band appearing between the 2000 and 3000 bp markers, as amplification of HV-1 does. The PCR result of HV-1 indicates that the transposon was inserted into the *zpx* gene. This difference in size of the wild type *zpx* gene and the *zpx*::Tn5 gene is clearly visible on gel electrophoresis (Figure 8).

Our study developed two unique site-specific mutagenesis procedures of varying success; one involving bacteriophage infection and the other utilizing linear transformation via electroporation. Both procedures targeted the *zpx* gene of *C. sakazakii* and involved cloning into a plasmid vector, treatment with a random transposon insertion kit, and selection of the *zpx*::Tn5 gene. The selection of the *zpx*::Tn5 gene was performed through PCR screening and selection of an amplicon that had a larger size than that of the wild type *zpx* amplification size, indicating that the random insertion kit had inserted the transposon into the *zpx* gene in the plasmid vector. The main obstacle occurred after attempting to transfer the mutated *zpx* gene that was present in an *E. coli* host into the wild type *C. sakazakii* strain CT2 to replace its wild type *zpx.*

Our first attempt involved infecting the *E. coli* culture containing *zpx*::Tn5 with pCRE1 bacteriophage. The bacteriophage lysed the *E. coli* and randomly packaged host DNA into its capsid, including the mutated *zpx*. Initial attempts of infecting non-competent wild type *C. sakazakii* cells with the phage lysate in a straight-forward transduction procedure met with failure, which led to alterations in the procedure. The phage lysate was transformed into chemically competent wild type *C. sakazakii* in an attempt to replace the wild type *zpx* gene with the *zpx*::Tn5 gene through homologous recombination.

Amplification of the *zpx* gene of EW-1 using Esak 5P and ES-R2 primers (Table 1) resulted in two distinctive bands (Figure 8); one the size of the wild type *zpx* of CT2 and another

that was the size of the *zpx*::Tn5 gene of HV-1. This indicates that both the wild type and the *zpx*::Tn5 gene were present in EW-1. The PCR results could imply that *zpx*::Tn5 gene was either incorporated into the genome following a single cross over event, or that the vector re-circularized after transformation. In order to further confirm that EW-1 possessed the transposon inserted *zpx* gene, two PCR reactions were performed using a grouping of the forward *zpx* gene primer along with the reverse transposon primer and vise versa (Table 2). These amplification of these primer grouping produced two amplicons whose sizes add up to equal that of the wild type *zpx* and the Tn5. This confirms that the transposon was indeed inserted into the *zpx* of EW-1. A single cross over event would have resulted in a merodiploid *zpx;* this would mean that the pGEM plasmid was also incorporated into the genome of *C. sakazakii*.

The HV-1 plasmid isolation resulted in a plasmid size just below 6000 bp. This was the pGEM vector (3015 bp) with the *zpx*::Tn5 gene (2247 bp) resulting in a final size of 5262 bp. The plasmid isolation of the pCRE1-infected *C. sakazakii,* EW-1, indicated that there was no difference in the plasmids from that of the wild type and that the pGEM vector was not present (Figure 9). These results help confirm that EW-1 was most likely indeed merodiploid for *zpx,* meaning that EW-1 contains two copies of the same gene in its genome. Figure 6 illustrates one possible merodiploid *zpx* in *C. sakazakii* as well as the primers used and their amplification directions. The double crossover event would have completely replaced the wild type *zpx* and incorporated the mutated *zpx* into the *C. sakazakii* genome. However, a single crossover event would result in the incorporation of the *zpx*::Tn5 gene into the genome along with the already-present wild type gene. The *zpx*::Tn5 gene was incorporated to the *C. sakazakii* genome, but failed a double cross over. Overall, the transduction procedure was not able to replace the wild type gene completely in *C. sakazakii,* which led to the development of the second procedure.

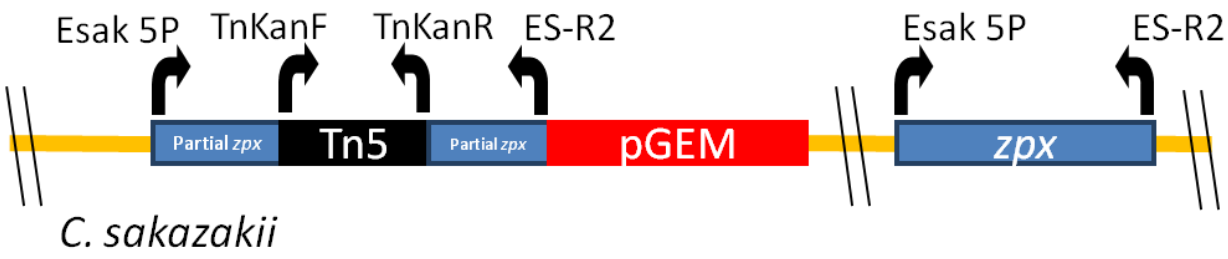

Figure 6. Merodiploid zpx in *C. sakazakii* CT2. One possible orientation of multiple zpx genes in C. sakazakii following transformation of the phage lysate. Primer locations are identified as well.

The results of the initial transduction mutagenesis procedure led to the development of a second site-specific mutagenesis procedure. This second procedure used electroporation to transform the amplified *zpx*::Tn5 gene of HV-1 into electro-competent *C. sakazakii* cells. The PCR results indicated that only the mutated *zpx* (2247 bp) was present, with no presence of the wild type (1026 bp) (Figure 8). Amplification of the *zpx* gene of EW-A (Table 1) resulted in only a single band that was the same size as the *zpx*::Tn5 gene of HV-1 (Figure 8). There was no presence of the wild type *zpx* gene after amplification. Only the larger, *zpx*::Tn5 amplicon, was visible. This likely indicates that the *zpx*::Tn5 gene successfully replaced the wild type *zpx* completely. Plasmid isolation of EW-A revealed no additional plasmids similar to that of the wild type *C. sakazakii* and no presence of the pGEM vector (Figure 9). These plasmid isolation results help conclude that the pZpx simply did not just re-circularize after transformation and that the *zpx*::Tn5 gene was now incorporated into the host's genome.

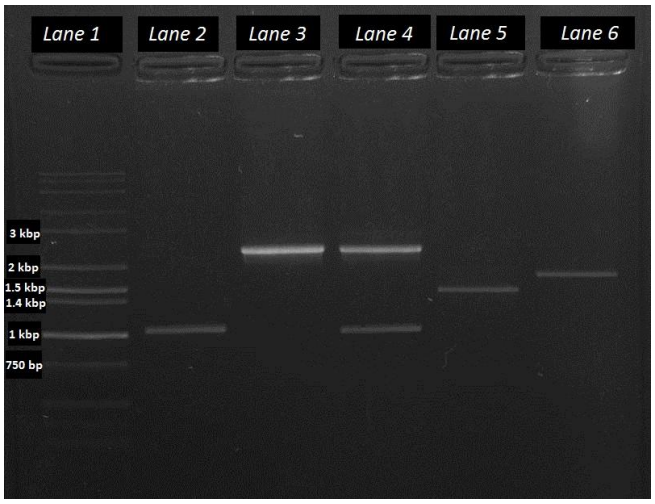

Figure 7. Merodiploid verification. Lane 1 Hi-Lo DNA Marker. Lane 2 Wild type *C. sakazakii* strain CT2 *zpx* amplicon. Lane 3 *zpx* amplicon from the *E. coli* HV-1. Lane 4 *zpx* amplicon from EW-1. Lane 5 Amplicons from Esak 5P and TnKanR primer grouping. Lane 6 Amplicons from ES-R2 and TnKanF primer grouping.

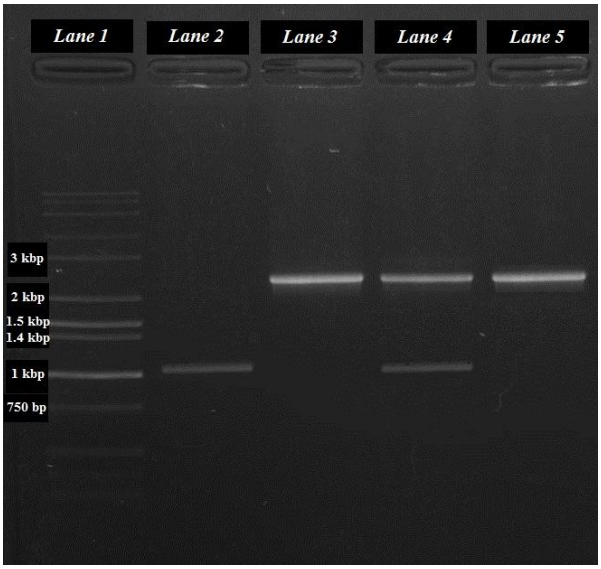

Figure 8. *zpx* PCR amplification**.** Lane 1 Hi-Lo DNA Marker. Lane 2 Wild type *C. sakazakii* strain CT2 *zpx* amplicon. Lane 3 *zpx* amplicon from the *E. coli* HV-1. Lane 4 *zpx* amplicon from EW-1. Lane 5 *zpx* amplicon from EW-A.

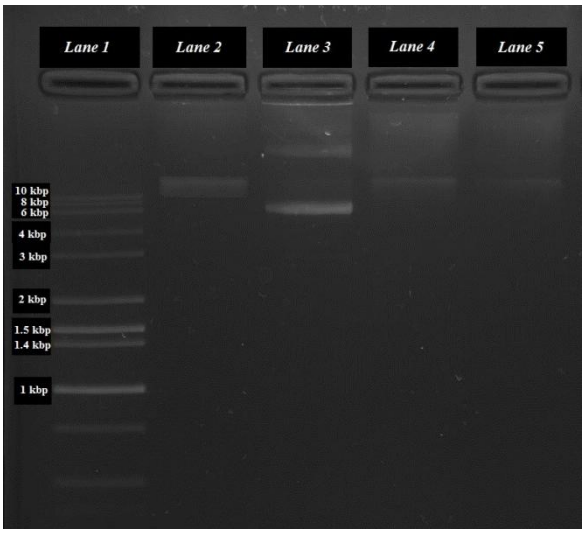

Figure 9. Plasmid isolation. Lane 1 Hi-Lo DNA Marker. Lane 2 Wild type *C. sakazakii* strain CT2 plasmid. Lane 3 Plasmid isolated from *E. coli* HV-1. Lane 4 Plasmid from EW-1. Lane 5 Plasmid from EW-A.

Conclusion and Future Research

This study utilized a functional *in vitro* co-culture model of the BBB using mouse endothelial and astrocyte cells. The percent change UAR results indicate a significant difference between the positive and negative controls. This is further evidence that this model is feasible for investigation of *Cronobacter* pathogenesis under the parameters in this study. This study also developed a novel site-specific mutagenesis procedure to induce a mutation in putative virulence genes of *C. sakazakii*. Our results indicate that this mutagenesis procedure successfully induced a mutation in the *zpx* gene of wild type *C. sakazakii* CT2 strain as confirmed by PCR amplification (Figure 8) and plasmid isolation (Figure 9). However, additional characterization of this mutated gene is still needed. Sequencing of the mutated gene needs to be completed in the future. In addition, the EW-A mutant strain needs to be assessed for possible remain functionality of the transposon inserted *zpx* gene.

This linear transformation procedure could be used in the future to induce a mutation in other putative virulence genes of *C. sakazakii*. The *Cronobacter* plasminogen activator gene (*cpa*) described by Franco et al. would be an excellent target for further pathogenic research into this genus [26]. Additionally, the genes encoding a siderophore-interacting protein (*sip*) and the type III hemolysin (*hly*) described by Cruz et al. would also be feasible targets for further research [83]. This mutagenesis procedure could also be attempted on other species of the genus *Cronobacter* or possibly other bacteria within the family *Enterobacteriaceae* to determine its capability.

The issue of lower resistance of treatments located on the edges of the 24 well plates can be remedied in future studies. Noticeable discrepancies in resistance values solely because of placement in the well plate likely arose due to the difference in humidity and temperature during incubation. Future studies should only have treatments located in the center of the 24 well plates. Clustering treatments towards the middle of the plate will help standardize the temperature and humidity experienced in the study. Additionally, as the time between TEER measurements for each treatment can be lengthy, it would be prudent to only remove treatments right before they are to be read from the incubator and swiftly replaced after.

A co-culture model of the BBB used to investigate the virulence of this organism has only been documented in the thesis of Erin Koval [47]. Although there have been numerous studies performed to investigate *Cronobacter* pathogenesis using endothelial cells, a study has not been performed using both endothelial and astrocyte cells. Additionally, a virulence study of a *C. sakazakii* strain isolated from bovine feces is not documented in the available literature. In the future, the site-specific mutagenesis procedure using linear transformation could be used in conjunction with the co-culture BBB model to further investigate the pathogenesis of

Cronobacter sakazakii. According to the Duncan's Multiple Range Test results, we could potentially replace the negative control in our model with BAA-894, as they were not significantly different from one another after 24 hours. Additionally, the positive control could be replaced with N72, as they were also not significantly different from one another. This change would be most prudent if the model is to be used to further investigate the pathogenesis of *C. sakazakii*. The negative and positive controls used in this study were both *E. coli* and replacing them with *C. sakazakii* strains would improve the model using a direct comparison for investigating *Cronobacter* pathogenesis.

REFERENCES

1. Iversen, C., et al., *The taxonomy of Enterobacter sakazakii: proposal of a new genus Cronobacter gen. nov. and descriptions of Cronobacter sakazakii comb. nov. Cronobacter sakazakii subsp. sakazakii, comb. nov., Cronobacter sakazakii subsp. malonaticus subsp. nov., Cronobacter turicensis sp. nov., Cronobacter muytjensii sp. nov., Cronobacter dublinensis sp. nov. and Cronobacter genomospecies 1.* BMC Evol Biol, 2007. **7**: p. 64.
2. Farmer, J.J., 3rd, et al., *Enterobacter sakazakii: A New Species of "Enterobacteriaceae" Isolated from Clinical Specimens.* Int J Syst Bacteriology, 1980. **30**(3): p. 569-584.
3. Jarvis, K.G., et al., *Identification and Characterization of Five New Molecular Serogroups of Cronobacter spp.* Foodborne Pathog Dis, 2013. **10**(4): p. 343-352.
4. Masood, N., et al., *Draft Genome Sequences of Three Newly Identified Species in the Genus Cronobacter, C. helveticus LMG23732T, C. pulveris LMG24059, and C. zurichensis LMG23730T.* Genome Announc, 2013. **1**(5).
5. Lai, K.K., *Enterobacter sakazakii infections among neonates, infants, children, and adults. Case reports and a review of the literature.* Medicine (Baltimore), 2001. **80**(2): p. 113-22.
6. van Acker, J., et al., *Outbreak of necrotizing enterocolitis associated with Enterobacter sakazakii in powdered milk formula.* J Clin Microbiol, 2001. **39**(1): p. 293-7.
7. Nazarowec-White, M. and J.M. Farber, *Enterobacter sakazakii: a review.* Int J Food Microbiol, 1997. **34**(2): p. 103-13.
8. Reich, F., et al., *Prevalence of Cronobacter spp. in a powdered infant formula processing environment.* Int J Food Microbiol, 2010. **140**(2-3): p. 214-7.

9. Simmons, B.P., et al., *Enterobacter sakazakii Infections in Neonates Associated with Intrinsic Contamination of a Powdered Infant Formula.* Infection Control and Hospital Epidemiology, 1989. **10**(9): p. 398-401.

10. Block, C., et al., *Cluster of neonatal infections in Jerusalem due to unusual biochemical variant of Enterobacter sakazakii.* Eur J Clin Microbiol Infect Dis, 2002. **21**(8): p. 613-6.

11. Himelright, I., *Enterobacter sakazakii infections associated with the use of powdered infant formula-Tennessee, 2001.* J. Am. Med. Assoc., 2002. **287**: p. 2204-2205.

12. Friedemann, M., *Enterobacter sakazakii in food and beverages (other than infant formula and milk powder).* Int J Food Microbiol, 2007. **116**(1): p. 1-10.

13. Jaradat, Z.W., et al., *Isolation of Cronobacter spp. (formerly Enterobacter sakazakii) from infant food, herbs and environmental samples and the subsequent identification and confirmation of the isolates using biochemical, chromogenic assays, PCR and 16S rRNA sequencing.* BMC Microbiol, 2009. **9**: p. 225.

14. Molloy, C., et al., *Surveillance and characterisation by pulsed-field gel electrophoresis of Cronobacter spp. in farming and domestic environments, food production animals and retail foods.* Int J Food Microbiol, 2009. **136**(2): p. 198-203.

15. Kandhai, M.C., et al., *Occurrence of Enterobacter sakazakii in food production environments and households.* Lancet, 2004. **363**(9402): p. 39-40.

16. Schmid, M., et al., *Evidence for a plant-associated natural habitat for Cronobacter spp.* Res Microbiol, 2009. **160**(8): p. 608-14.

17. Lehner, A., et al., *Biofilm formation, extracellular polysaccharide production, and cell-to-cell signaling in various Enterobacter sakazakii strains: aspects promoting environmental persistence.* J Food Prot, 2005. **68**(11): p. 2287-94.

18. Townsend, S., et al., *The presence of endotoxin in powdered infant formula milk and the influence of endotoxin and Enterobacter sakazakii on bacterial translocation in the infant rat.* Food Microbiol, 2007. **24**(1): p. 67-74.

19. Pagotto, F.J., et al., *Enterobacter sakazakii: infectivity and enterotoxin production in vitro and in vivo.* J Food Prot, 2003. **66**(3): p. 370-5.

20. Giri, C.P., et al., *Cronobacter spp. (previously Enterobacter sakazakii) invade and translocate across both cultured human intestinal epithelial cells and human brain microvascular endothelial cells.* Microb Pathog, 2012. **52**(2): p. 140-7.

21. Mange, J.P., et al., *Adhesive properties of Enterobacter sakazakii to human epithelial and brain microvascular endothelial cells.* BMC Microbiol, 2006. **6**: p. 58.

22. Singamsetty, V.K., et al., *Outer membrane protein A expression in Enterobacter sakazakii is required to induce microtubule condensation in human brain microvascular endothelial cells for invasion.* Microb Pathog, 2008. **45**(3): p. 181-91.

23. Khan, N.A., et al., *Outer membrane protein A and cytotoxic necrotizing factor-1 use diverse signaling mechanisms for Escherichia coli K1 invasion of human brain microvascular endothelial cells.* Microb Pathog, 2003. **35**(1): p. 35-42.

24. Sukumaran, S.K. and N.V. Prasadarao, *Escherichia coli K1 invasion increases human brain microvascular endothelial cell monolayer permeability by disassembling vascular-endothelial cadherins at tight junctions.* J Infect Dis, 2003. **188**(9): p. 1295-309.

25. Prasadarao, N.V., et al., *Outer membrane protein A of Escherichia coli contributes to invasion of brain microvascular endothelial cells.* Infect Immun, 1996. **64**(1): p. 146-53.

26. Franco, A., et al., *Cpa, the outer membrane protease of Cronobacter sakazakii, activates plasminogen and mediates resistance to serum bactericidal activity.* Infection and immunity, 2011. **79**(4): p. 1578-1587.

27. Kothary, M.H., et al., *Characterization of the zinc-containing metalloprotease encoded by zpx and development of a species-specific detection method for Enterobacter sakazakii.* Appl Environ Microbiol, 2007. **73**(13): p. 4142-51.

28. Healy, B., et al., *Cronobacter (Enterobacter sakazakii): an opportunistic foodborne pathogen.* Foodborne Pathog Dis, 2010. **7**(4): p. 339-50.

29. Hunter, C.J. and J.F. Bean, *Cronobacter: an emerging opportunistic pathogen associated with neonatal meningitis, sepsis and necrotizing enterocolitis.* J Perinatol, 2013.

30. Urmenyi, A.M. and A.W. Franklin, *Neonatal death from pigmented coliform infection.* Lancet, 1961. **1**(7172): p. 313-5.

31. Iversen, C. and S.J. Forsythe, *Comparison of media for the isolation of Enterobacter sakazakii.* Appl Environ Microbiol, 2007. **73**(1): p. 48-52.

32. Johler, S., et al., *Genes involved in yellow pigmentation of Cronobacter sakazakii ES5 and influence of pigmentation on persistence and growth under environmental stress.* Appl Environ Microbiol, 2010. **76**(4): p. 1053-61.

33. Iversen, C., et al., *Cronobacter gen. nov., a new genus to accommodate the biogroups of Enterobacter sakazakii, and proposal of Cronobacter sakazakii gen. nov., comb. nov., Cronobacter malonaticus sp. nov., Cronobacter turicensis sp. nov., Cronobacter muytjensii sp. nov., Cronobacter dublinensis sp. nov., Cronobacter genomospecies 1, and of three subspecies, Cronobacter dublinensis subsp. dublinensis subsp. nov., Cronobacter*

dublinensis subsp. lausannensis subsp. nov. and Cronobacter dublinensis subsp. lactaridi subsp. nov. Int J Syst Evol Microbiol, 2008. **58**(Pt 6): p. 1442-7.

34. Belal, M., et al., *Detection of Cronobacter spp. (formerly Enterobacter sakazakii) from medicinal plants and spices in Syria.* J Infect Dev Ctries, 2013. **7**(2): p. 82-9.

35. Lehner, A. and R. Stephan, *Microbiological, epidemiological, and food safety aspects of Enterobacter sakazakii.* J Food Prot, 2004. **67**(12): p. 2850-7.

36. Bar-Oz, B., et al., *Enterobacter sakazakii infection in the newborn.* Acta Paediatr, 2001. **90**(3): p. 356-8.

37. Clark, N.C., et al., *Epidemiologic typing of Enterobacter sakazakii in two neonatal nosocomial outbreaks.* Diagn Microbiol Infect Dis, 1990. **13**(6): p. 467-72.

38. Farber, J.M., S.J. Forsythe, and A.S.f. Microbiology, *Enterobacter Sakazakii*. 2008: Amer Society for Microbiology.

39. Corti, G., et al., *Postsurgical osteomyelitis caused by Enterobacter sakazakii in a healthy young man.* J Chemother, 2007. **19**(1): p. 94-6.

40. Caubilla-Barron, J., et al., *Genotypic and phenotypic analysis of Enterobacter sakazakii strains from an outbreak resulting in fatalities in a neonatal intensive care unit in France.* J Clin Microbiol, 2007. **45**(12): p. 3979-85.

41. Assadi, M.M. and R.P. Mathur, *Applicability of an HPLC System in the Analysis of Biodegraded Crude Oil Components.* Journal of Liquid Chromatography, 1991. **14**(19): p. 3623-3629.

42. Espeland, E.M. and R.G. Wetzel, *Complexation, Stabilization, and UV Photolysis of Extracellular and Surface-Bound Glucosidase and Alkaline Phosphatase: Implications for Biofilm Microbiota.* Microb Ecol, 2001. **42**(4): p. 572-585.

43. Gakuya, F.M., et al., *Antimicrobial resistance of bacterial organisms isolated from rats.* East Afr Med J, 2001. **78**(12): p. 646-9.

44. Kuzina, L.V., et al., *Isolation and identification of bacteria associated with adult laboratory Mexican fruit flies, Anastrepha ludens (Diptera: Tephritidae).* Curr Microbiol, 2001. **42**(4): p. 290-4.

45. Mramba, F., A. Broce, and L. Zurek, *Isolation of Enterobacter sakazakii from stable flies, Stomoxys calcitrans L. (Diptera: Muscidae).* J Food Prot, 2006. **69**(3): p. 671-3.

46. Neelam, M., Z. Nawaz, and S. Riazuddin, *Hydrocarbon biodegradation: Biochemical characterization of bacteria isolated from local soils.* Pakistan Journal of Scientific and Industrial Research, 1987. **30**(5): p. 382-385.

47. Koval, E., *An in-vitro co-culture model to study the disruption of the blood brain barrier by cronobacter sakazakii (formally enterobacter sakazakii)*, in *Agriculture and Applied Science*. 2010, North Dakota State University: Fargo, ND. p. 57.

48. Barron, J.C. and S.J. Forsythe, *Dry stress and survival time of Enterobacter sakazakii and other Enterobacteriaceae in dehydrated powdered infant formula.* Journal of food protection, 2007. **70**(9): p. 2111.

49. Kandhai, M.C., et al., *Effects of preculturing conditions on lag time and specific growth rate of Enterobacter sakazakii in reconstituted powdered infant formula.* Appl Environ Microbiol, 2006. **72**(4): p. 2721-9.

50. Iversen, C., M. Lane, and S.J. Forsythe, *The growth profile, thermotolerance and biofilm formation of Enterobacter sakazakii grown in infant formula milk.* Lett Appl Microbiol, 2004. **38**(5): p. 378-82.

51. Kandhai, M., et al., *Effects of preculturing conditions on lag time and specific growth rate of Enterobacter sakazakii in reconstituted powdered infant formula.* Applied and environmental microbiology, 2006. **72**(4): p. 2721-2729.

52. Iversen, C., P. Druggan, and S. Forsythe, *A selective differential medium for Enterobacter sakazakii, a preliminary study.* Int J Food Microbiol, 2004. **96**(2): p. 133-9.

53. Barron, J.C. and S.J. Forsythe, *Dry stress and survival time of Enterobacter sakazakii and other Enterobacteriaceae in dehydrated powdered infant formula.* J Food Prot, 2007. **70**(9): p. 2111-7.

54. Breeuwer, P., et al., *Desiccation and heat tolerance of Enterobacter sakazakii.* J Appl Microbiol, 2003. **95**(5): p. 967-73.

55. Gurtler, J.B. and L.R. Beuchat, *Survival of Enterobacter sakazakii in powdered infant formula as affected by composition, water activity, and temperature.* J Food Prot, 2007. **70**(7): p. 1579-86.

56. Kim, S.H. and J.H. Park, *Thermal resistance and inactivation of Enterobacter sakazakii isolates during rehydration of powdered infant formula.* J Microbiol Biotechnol, 2007. **17**(2): p. 364-8.

57. Kempf, B. and E. Bremer, *Uptake and synthesis of compatible solutes as microbial stress responses to high-osmolality environments.* Arch Microbiol, 1998. **170**(5): p. 319-30.

58. Bhat, G.K., et al., *Urinary tract infection due to Enterobacter sakazakii.* Indian J Pathol Microbiol, 2009. **52**(3): p. 430-1.

59. Frantz Iii, I.D., et al., *Necrotizing enterocolitis.* The Journal of Pediatrics, 1975. **86**(2): p. 259-263.

60. Shah, U. and W. Walker, *Adverse host responses to bacterial toxins in human infants.* The Journal of nutrition, 2000. **130**(2): p. 420S-425S.

61. Townsend, S.M., et al., *Enterobacter sakazakii invades brain capillary endothelial cells, persists in human macrophages influencing cytokine secretion and induces severe brain pathology in the neonatal rat.* Microbiology, 2007. **153**(Pt 10): p. 3538-47.

62. Gallagher, P.G. and W.S. Ball, *Cerebral infarctions due to CNS infection with Enterobacter sakazakii.* Pediatr Radiol, 1991. **21**(2): p. 135-6.

63. Bowen, A.B. and C.R. Braden, *Invasive Enterobacter sakazakii disease in infants.* Emerg Infect Dis, 2006. **12**(8): p. 1185-9.

64. Stevens, J.P., et al., *Long term outcome of neonatal meningitis.* Arch Dis Child Fetal Neonatal Ed, 2003. **88**(3): p. F179-84.

65. Harvey, D., D.E. Holt, and H. Bedford, *Bacterial meningitis in the newborn: a prospective study of mortality and morbidity.* Semin Perinatol, 1999. **23**(3): p. 218-25.

66. Chenu, J.W. and J.M. Cox, *Cronobacter ('Enterobacter sakazakii'): current status and future prospects.* Lett Appl Microbiol, 2009. **49**(2): p. 153-9.

67. Willis, J. and J.E. Robinson, *Enterobacter sakazakii meningitis in neonates.* Pediatr Infect Dis J, 1988. **7**(3): p. 196-9.

68. Wolff, M.A., C.L. Young, and R. Ramphal, *Antibiotic therapy for enterobacter meningitis: a retrospective review of 13 episodes and review of the literature.* Clin Infect Dis, 1993. **16**(6): p. 772-7.

69. Kramer, M. and R. Kakuma, *Optimal duration of exclusive breastfeeding (Review).* 2009.

70. Muytjens, H.L., et al., *Analysis of eight cases of neonatal meningitis and sepsis due to Enterobacter sakazakii.* J Clin Microbiol, 1983. **18**(1): p. 115-20.

71. *Enterobacter sakazakii infections associated with the use of powdered infant formula--Tennessee, 2001*. MMWR Morb Mortal Wkly Rep, 2002. **51**(14): p. 297-300.

72. Norberg, S., et al., *Cronobacter spp. in powdered infant formula.* J Food Prot, 2012. **75**(3): p. 607-20.

73. Hunter, C.J. and J.F. Bean, *Cronobacter: an emerging opportunistic pathogen associated with neonatal meningitis, sepsis and necrotizing enterocolitis.* J Perinatol, 2013. **33**(8): p. 581-5.

74. Stoll, B.J., et al., *Enterobacter sakazakii is a rare cause of neonatal septicemia or meningitis in VLBW infants.* J Pediatr, 2004. **144**(6): p. 821-3.

75. Dennison, S.K. and J. Morris, *Multiresistant Enterobacter sakazakii wound infection in an adult.* Infections in medicine, 2002. **19**(11): p. 533-535.

76. Hawkins, R.E., C.R. Lissner, and J.P. Sanford, *Enterobacter sakazakii bacteremia in an adult.* South Med J, 1991. **84**(6): p. 793-5.

77. LAI, K.K., *Enterobacter sakazakii Infections among Neonates, Infants, Children, and Adults: Case Reports and a Review of the Literature.* Medicine, 2001. **80**(2): p. 113-122.

78. Ongradi, J., *Vaginal infection by Enterobacter sakazakii.* Sexually transmitted infections, 2002. **78**(6): p. 467-467.

79. Brand, B., *Kimberly-clark recalls kotex natural balance security unscented tampons regular absorbency from a limited number of retail stores within the united states*. 2011, U.S. Food and Drug Administration: http://www.fda.gov/safety/recalls/ucm279588.htm.

80. Hartmann, I., et al., *Genes involved in Cronobacter sakazakii biofilm formation.* Appl Environ Microbiol, 2010. **76**(7): p. 2251-61.

81. Kim, H., J.H. Ryu, and L.R. Beuchat, *Attachment of and biofilm formation by Enterobacter sakazakii on stainless steel and enteral feeding tubes.* Appl Environ Microbiol, 2006. **72**(9): p. 5846-56.

82. Hall-Stoodley, L., J.W. Costerton, and P. Stoodley, *Bacterial biofilms: from the natural environment to infectious diseases.* Nat Rev Microbiol, 2004. **2**(2): p. 95-108.

83. Cruz, A., et al., *Virulence traits in Cronobacter species isolated from different sources.* Can J Microbiol, 2011. **57**(9): p. 735-44.

84. Scheepe-Leberkühne, M. and F. Wagner, *Optimization and preliminary characterization of an exopolysaccharide synthezised by Enterobacter sakazakii.* Biotechnology Letters, 1986. **8**(10): p. 695-700.

85. Kim, K.P. and M.J. Loessner, *Enterobacter sakazakii invasion in human intestinal Caco-2 cells requires the host cell cytoskeleton and is enhanced by disruption of tight junction.* Infect Immun, 2008. **76**(2): p. 562-70.

86. Hunter, C.J., et al., *Enterobacter sakazakii enhances epithelial cell injury by inducing apoptosis in a rat model of necrotizing enterocolitis.* J Infect Dis, 2008. **198**(4): p. 586-93.

87. Wilhelm, I., C. Fazakas, and I.A. Krizbai, *In vitro models of the blood-brain barrier.* Acta Neurobiol Exp (Wars), 2011. **71**(1): p. 113-28.

88. Kucerova, E., et al., *Genome sequence of Cronobacter sakazakii BAA-894 and comparative genomic hybridization analysis with other Cronobacter species.* PLoS One, 2010. **5**(3): p. e9556.

89. Stephan, R., et al., *Complete genome sequence of Cronobacter turicensis LMG 23827, a food-borne pathogen causing deaths in neonates.* J Bacteriol, 2011. **193**(1): p. 309-10.

90. Franco, A.A., et al., *Characterization of putative virulence genes on the related RepFIB plasmids harbored by Cronobacter spp.* Appl Environ Microbiol, 2011. **77**(10): p. 3255-67.

91. Franco, A.A., et al., *Cpa, the outer membrane protease of Cronobacter sakazakii, activates plasminogen and mediates resistance to serum bactericidal activity.* Infect Immun, 2011. **79**(4): p. 1578-87.

92. Pardridge, W.M., *Blood-brain barrier biology and methodology.* J Neurovirol, 1999. **5**(6): p. 556-69.

93. Ballabh, P., A. Braun, and M. Nedergaard, *The blood-brain barrier: an overview: structure, regulation, and clinical implications.* Neurobiol Dis, 2004. **16**(1): p. 1-13.

94. Janzer, R.C. and M.C. Raff, *Astrocytes induce blood-brain barrier properties in endothelial cells.* Nature, 1987. **325**(6101): p. 253-7.

95. Abbott, N.J., L. Ronnback, and E. Hansson, *Astrocyte-endothelial interactions at the blood-brain barrier.* Nat Rev Neurosci, 2006. **7**(1): p. 41-53.

96. Dore-Duffy, P., *Pericytes: pluripotent cells of the blood brain barrier.* Curr Pharm Des, 2008. **14**(16): p. 1581-93.

97. Armulik, A., et al., *Pericytes regulate the blood-brain barrier.* Nature, 2010. **468**(7323): p. 557-61.

98. Persidsky, Y., et al., *Blood-brain barrier: structural components and function under physiologic and pathologic conditions.* J Neuroimmune Pharmacol, 2006. **1**(3): p. 223-36.

99. Ebnet, K., et al., *Junctional adhesion molecules (JAMs): more molecules with dual functions?* J Cell Sci, 2004. **117**(Pt 1): p. 19-29.

100. Nicolazzo, J.A., S.A. Charman, and W.N. Charman, *Methods to assess drug permeability across the blood-brain barrier.* J Pharm Pharmacol, 2006. **58**(3): p. 281-93.

101. Brocato, R.L. and T.G. Voss, *Pichinde virus induces microvascular endothelial cell permeability through the production of nitric oxide.* Virol J, 2009. **6**: p. 162.

102. Butt, A.M., H.C. Jones, and N.J. Abbott, *Electrical resistance across the blood-brain barrier in anaesthetized rats: a developmental study.* J Physiol, 1990. **429**: p. 47-62.

103. Deli, M.A., et al., *Permeability studies on in vitro blood-brain barrier models: physiology, pathology, and pharmacology.* Cell Mol Neurobiol, 2005. **25**(1): p. 59-127.

104. Demeuse, P., et al., *Compartmentalized coculture of rat brain endothelial cells and astrocytes: a syngenic model to study the blood-brain barrier.* J Neurosci Methods, 2002. **121**(1): p. 21-31.

105. Lauer, R., et al., *Development of an in vitro blood-brain barrier model based on immortalized porcine brain microvascular endothelial cells.* Farmaco, 2004. **59**(2): p. 133-7.

106. Li, G., et al., *Permeability of endothelial and astrocyte cocultures: in vitro blood-brain barrier models for drug delivery studies.* Ann Biomed Eng, 2010. **38**(8): p. 2499-511.

107. Ma, S.H., et al., *An endothelial and astrocyte co-culture model of the blood-brain barrier utilizing an ultra-thin, nanofabricated silicon nitride membrane.* Lab Chip, 2005. **5**(1): p. 74-85.

108. Matter, K. and M.S. Balda, *Signalling to and from tight junctions.* Nat Rev Mol Cell Biol, 2003. **4**(3): p. 225-36.

109. Nakagawa, S., et al., *A new blood-brain barrier model using primary rat brain endothelial cells, pericytes and astrocytes.* Neurochem Int, 2009. **54**(3-4): p. 253-63.

110. Toimela, T., et al., *Development of an in vitro blood-brain barrier model-cytotoxicity of mercury and aluminum.* Toxicol Appl Pharmacol, 2004. **195**(1): p. 73-82.

111. Liu, Q., et al., *Human isolates of Cronobacter sakazakii bind efficiently to intestinal epithelial cells in vitro to induce monolayer permeability and apoptosis.* J Surg Res, 2012. **176**(2): p. 437-47.

112. Hart, M.N., et al., *Differential opening of the brain endothelial barrier following neutralization of the endothelial luminal anionic charge in vitro.* J Neuropathol Exp Neurol, 1987. **46**(2): p. 141-53.

113. Rutten, M.J., R.L. Hoover, and M.J. Karnovsky, *Electrical resistance and macromolecular permeability of brain endothelial monolayer cultures.* Brain Res, 1987. **425**(2): p. 301-10.

114. Maruyama, I.N. and S. Brenner, *A selective lambda phage cloning vector with automatic excision of the insert in a plasmid.* Gene, 1992. **120**(2): p. 135-41.

115. Gaillard, P.J., et al., *Establishment and functional characterization of an in vitro model of the blood–brain barrier, comprising a co-culture of brain capillary endothelial cells and astrocytes.* European Journal of Pharmaceutical Sciences, 2001. **12**(3): p. 215-222.

APPENDIX

Table A1. Plate 1 raw TEER data

Plate 1 A

Unit Area Resistance (Ω * cm^2)

Time						
0hr	Blank	N72	N72	BAA-894	Negative	Positive
	30.6	72.9	67.8	66.9	65.7	69.3
	Cells	71.1	67.2	65.4	66.9	61.5
	69.9	74.4	72	69.9	64.8	65.4
	73.8	70.5	69.9	67.2	66.3	69.3
24hr	Blank	N72	N72	BAA-894	Negative	Positive
	29.4	47.1	40.5	45	64.2	45
	Cells	45	41.1	47.7	62.1	41.1
	60.9	45.3	43.8	47.1	63	44.4
	65.7	44.1	45.9	43.5	60.6	49.2

Plate 1 B

Unit Area Resistance (Ω * cm2)

Time						
0hr	Blank	N72	BAA-894	BAA-894	Negative	Positive
	28.8	52.5	54	48	50.4	50.1
	Cells	66.6	57.6	59.4	49.5	51.9
	60.3	63	58.5	60.9	51.3	60.9
	57.9	58.2	56.7	58.5	58.5	60
24hr	Blank	N72	BAA-894	BAA-894	Negative	Positive
	27.9	44.4	35.1	41.7	47.7	34.2
	Cells	61.5	50.4	52.8	48.6	34.2
	56.7	43.2	53.7	52.8	51.9	43.5
	54.9	39	50.4	52.2	57.3	41.1

Table A2. Plate 2 raw TEER data

Plate 2 A

Unit Area Resistance ($\Omega * cm^2$)

Time						
0hr	Blank	N72	N72	BAA-894	Negative	Positive
	32.1	57	55.5	54.6	63.3	56.1
	Cells	57.6	60	56.1	57.6	59.1
	65.4	62.7	58.2	54.9	58.5	59.4
	61.2	62.1	53.1	55.5	53.1	57.3
24hr	Blank	N72	N72	BAA-894	Negative	Positive
	29.7	39.3	39.9	39.6	64.2	40.8
	Cells	37.5	37.2	43.5	52.5	38.1
	56.7	39	38.1	41.1	56.1	41.1
	53.7	37.2	37.5	40.5	51.9	41.1

Plate 2 B

Unit Area Resistance (Ω * cm2)

Time						
0hr	Blank	N72	BAA-894	BAA-894	Negative	Positive
	33.3	54.6	54	54	49.8	53.7
	Cells	57.3	61.8	53.4	54.9	53.4
	59.7	63.6	62.1	61.5	55.8	60
	56.1	58.2	59.7	58.2	56.1	57.3
24hr	Blank	N72	BAA-894	BAA-894	Negative	Positive
	28.5	40.5	37.5	39	51.9	38.4
	Cells	41.1	45	36.9	51.6	36.6
	52.2	39.9	42.6	41.4	48.9	41.4
	50.7	41.1	41.7	41.4	42.9	39.6

Table A3. Plate 3 raw TEER data

Plate 3 A

Unit Area Resistance ($\Omega * cm^2$)

Time	Blank	N72	N72	BAA-894	Negative	Positive
0hr						
	65.7	130.8	129.6	138.6	131.4	125.7
	Cells	143.7	126.6	132.9	129.3	118.8
	122.7	120	123.3	115.5	125.4	134.7
	138.3	127.2	127.8	132.9	131.4	120
24hr	Blank	N72	N72	BAA-894	Negative	Positive
	56.7	120.3	101.4	133.2	131.7	109.8
	Cells	124.5	103.8	126.6	134.7	101.7
	127.2	98.4	100.2	110.1	115.8	106.8
	120.6	110.4	110.1	133.5	112.5	108.6

Plate 3 B

Unit Area Resistance (Ω * cm2)

Time						
0hr	Blank	N72	BAA-894	BAA-894	Negative	Positive
	63.3	129.9	114.9	118.5	128.7	131.4
	Cells	134.7	131.1	123.3	119.4	135.3
	134.1	122.4	139.5	108.3	118.2	127.5
	131.4	134.7	130.5	109.2	111.9	119.7
24hr	Blank	N72	BAA-894	BAA-894	Negative	Positive
	57.3	108.9	119.7	114.3	129.3	115.5
	Cells	119.1	139.5	122.1	128.7	118.8
	120.9	120	135	100.5	121.5	110.1
	127.2	124.5	135.6	112.5	110.1	105.3

Table A4. Plate 4 raw TEER data

Plate 4 A

Unit Area Resistance ($\Omega * cm^2$)

Time						
0hr	Blank	N72	N72	BAA-894	Negative	Positive
	60	40.8	44.4	46.5	140.1	139.5
	Cells	166.2	130.8	52.8	137.7	42.9
	139.8	36.6	132	158.4	57.3	153.3
	135.3	153.9	42	41.4	141.3	40.2
24hr	Blank	N72	N72	BAA-894	Negative	Positive
	62.4	33.3	30.9	38.4	124.5	119.7
	Cells	151.5	105.9	44.7	130.8	21.6
	123.9	18.3	120.3	139.5	30.9	135.6
	129.6	129.9	31.5	34.5	126.6	21.3

Plate 4 B

Unit Area Resistance (Ω * cm2)

Time						
0hr	Blank	N72	BAA-894	BAA-894	Negative	Positive
	62.4	138.9	141.9	124.2	141.6	136.8
	Cells	148.8	141.3	147.9	143.4	142.8
	134.4	137.4	137.7	142.2	143.1	137.7
	140.1	140.1	153.3	150.6	150	146.1
24hr	Blank	N72	BAA-894	BAA-894	Negative	Positive
	59.4	124.5	123	121.5	130.8	112.5
	Cells	135.9	114.3	136.8	131.1	112.8
	127.8	127.8	108.3	130.8	132.3	111.6
	120.9	126.3	124.5	138	137.4	118.8

Table A5. Plate 5 raw TEER data

Plate 5 A

Unit Area Resistance ($\Omega * cm^2$)

Time						
0hr	Blank	N72	N72	BAA-894	Negative	Positive
	67.5	128.7	125.4	119.7	135.6	137.1
	Cells	123.6	122.1	123.9	127.2	126.6
	144.3	124.2	123	120.9	143.7	125.4
	130.2	121.2	130.5	133.8	134.7	131.7
24hr	Blank	N72	N72	BAA-894	Negative	Positive
	69.9	129.3	129.3	129	125.1	114.3
	Cells	123.3	125.7	144.9	111.6	112.5
	148.2	121.5	129.3	132.6	139.2	116.1
	134.4	123.3	143.1	144.6	119.1	118.5

Plate 5 B

Unit Area Resistance (Ω * cm2)

Time						
0hr	Blank	N72	BAA-894	BAA-894	Negative	Positive
	69.6	139.8	133.8	137.4	153.3	133.8
	Cells	142.8	143.4	133.5	143.4	137.1
	143.4	141.3	169.5	146.7	140.1	135.3
	146.7	138.6	137.1	141.3	133.8	134.4
24hr	Blank	N72	BAA-894	BAA-894	Negative	Positive
	66.9	140.1	138.3	150.9	143.4	128.4
	Cells	149.4	140.1	140.4	146.7	131.1
	139.5	138	160.5	152.7	146.7	143.1
	142.8	143.1	148.5	139.5	138.6	130.2

Table A6. Calculated percent change TEER data.

Observation	Plate Row	%Δh0-24	Treatment
1	1_Row1	0.69638	N72
2	1_Row2	0.72265	N72
3	1_Row3	0.63431	N72
4	1_Row4	0.68844	N72
5	2_Row1	0.71672	N72
6	2_Row2	0.66277	N72
7	2_Row3	0.63467	N72
8	2_Row4	0.67048	N72
9	3_Row1	0.84682	N72
10	3_Row2	0.85683	N72
11	3_Row3	0.87101	N72
12	3_Row4	0.88457	N72
13	4_Row1	0.80282	N72
14	4_Row2	0.87816	N72
15	4_Row3	0.78050	N72
16	4_Row4	0.83185	N72
17	5_Row1	1.01264	N72
18	5_Row2	1.02443	N72
19	5_Row3	1.00204	N72
20	5_Row4	1.04878	N72
21	1_Row1	0.73047	BAA-894
22	1_Row2	0.83108	BAA-894
23	1_Row3	0.81959	BAA-894
24	1_Row4	0.89938	BAA-894
25	2_Row1	0.71398	BAA-894

Table A6. Calculated percent change TEER data (continued).

Observation	Plate Row	%Δh0-24	Treatment
26	2_Row2	0.73152	BAA-894
27	2_Row3	0.70260	BAA-894
28	2_Row4	0.71319	BAA-894
29	3_Row1	0.98912	BAA-894
30	3_Row2	1.00231	BAA-894
31	3_Row3	0.94966	BAA-894
32	3_Row4	1.02460	BAA-894
33	4_Row1	0.89029	BAA-894
34	4_Row2	0.86015	BAA_894
35	4_Row3	0.86234	BAA-894
36	4_Row4	0.85393	BAA_894
37	5_Row1	1.06986	BAA-894
38	5_Row2	1.06605	BAA-894
39	5_Row3	1.02819	BAA-894
40	5_Row4	1.05038	BAA-894
41	1_Row1	0.96180	Negative
42	1_Row2	0.95503	Negative
43	1_Row3	0.99196	Negative
44	1_Row4	1.02210	Negative
45	2_Row1	1.02819	Negative
46	2_Row2	0.92567	Negative
47	2_Row3	0.91766	Negative
48	2_Row4	0.87105	Negative
49	3_Row1	1.00347	Negative
50	3_Row2	1.05983	Negative

Table A6. Calculated percent change TEER data (continued).

Observation	Plate Row	%Δh0-24	Treatment
51	3_Row3	0.97568	Negative
52	3_Row4	0.92004	Negative
53	4_Row1	0.90619	Negative
54	4_Row2	0.93206	Negative
55	4_Row3	0.73190	Negative
56	4_Row4	0.90598	Negative
57	5_Row1	0.92899	Negative
58	5_Row2	0.95019	Negative
59	5_Row3	1.00790	Negative
60	5_Row4	0.96003	Negative
61	1_Row1	0.66599	Positive
62	1_Row2	0.66363	Positive
63	1_Row3	0.69659	Positive
64	1_Row4	0.82096	Positive
65	2_Row1	0.72118	Positive
66	2_Row2	0.66503	Positive
67	2_Row3	0.69096	Positive
68	2_Row4	0.70419	Positive
69	3_Row1	0.87625	Positive
70	3_Row2	0.86705	Positive
71	3_Row3	0.82820	Positive
72	3_Row4	0.89235	Positive
73	4_Row1	0.84022	Positive
74	4_Row2	0.64671	Positive
75	4_Row3	0.84750	Positive

Table A6. Calculated percent change TEER data (continued).

Observation	Plate Row	%Δh0-24	Treatment
75	4_Row3	0.84750	Positive
76	4_Row4	0.67150	Positive
77	5_Row1	0.89667	Positive
78	5_Row2	0.92243	Positive
79	5_Row3	0.99174	Positive
80	5_Row4	0.93426	Positive

Table A7. The GLM procedure for %Δhour 0-24.

Class Level Information		
Class	Levels	Values
Treatment	4	BAA-894, N72, Negative, Positive

Source	DF	Sum of Squares	Mean Square	F Value	Pr > F
Model	3	0.30697412	0.10232471	7.89	0.0001
Error	76	0.98577626	0.01297074		
Corrected Total	79	1.29275039			

R-Square	Coeff Var	Root MSE	%Δ0-24 Mean
0.237458	13.23240	0.113889	0.860684

Source	DF	Type III SS	Mean Square	F Value	Pr > F
Treatment	3	0.30697412	0.10232471	7.89	0.0001

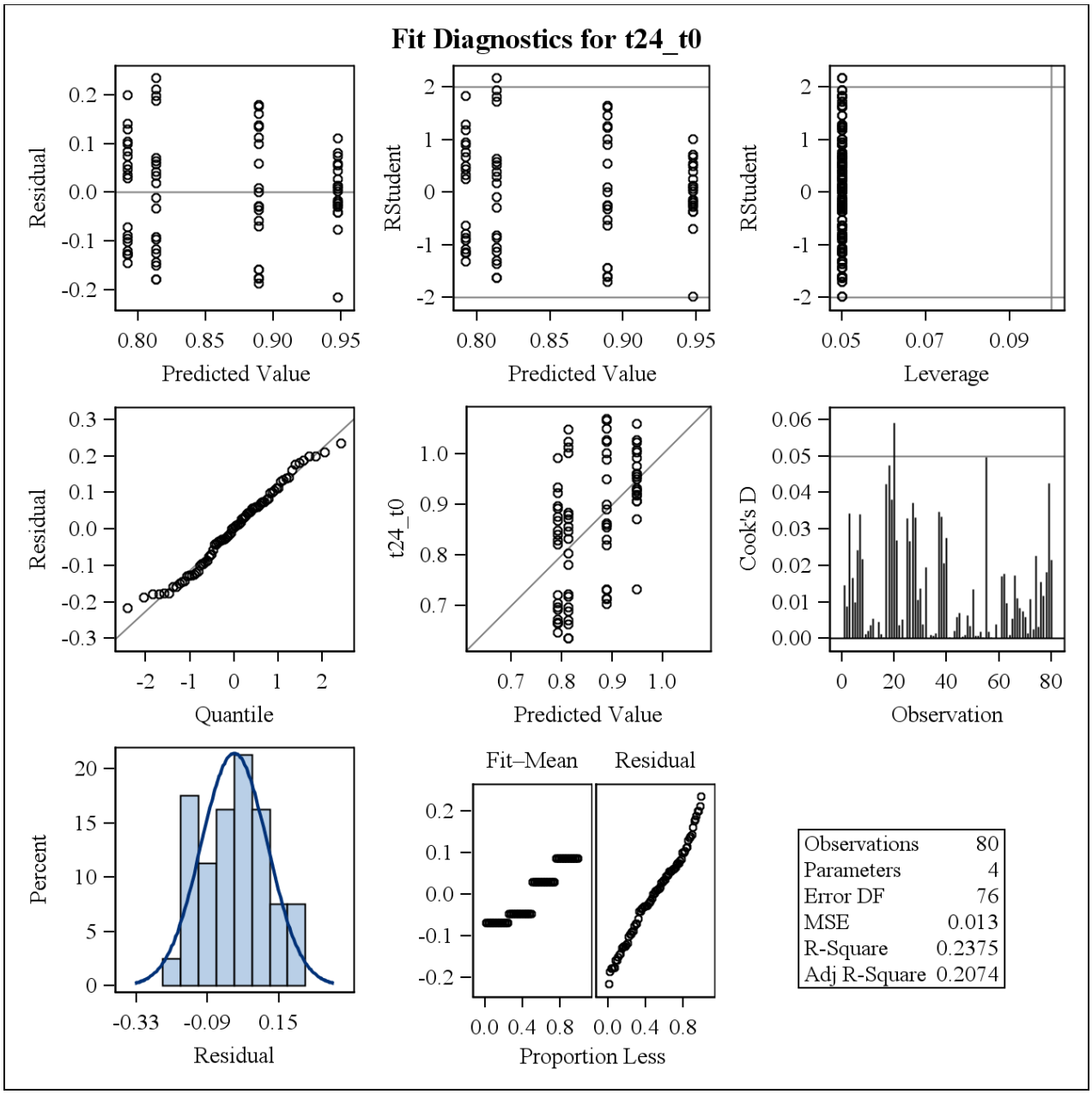

Figure A1. Fit diagnostics for %Δhour 0-24.

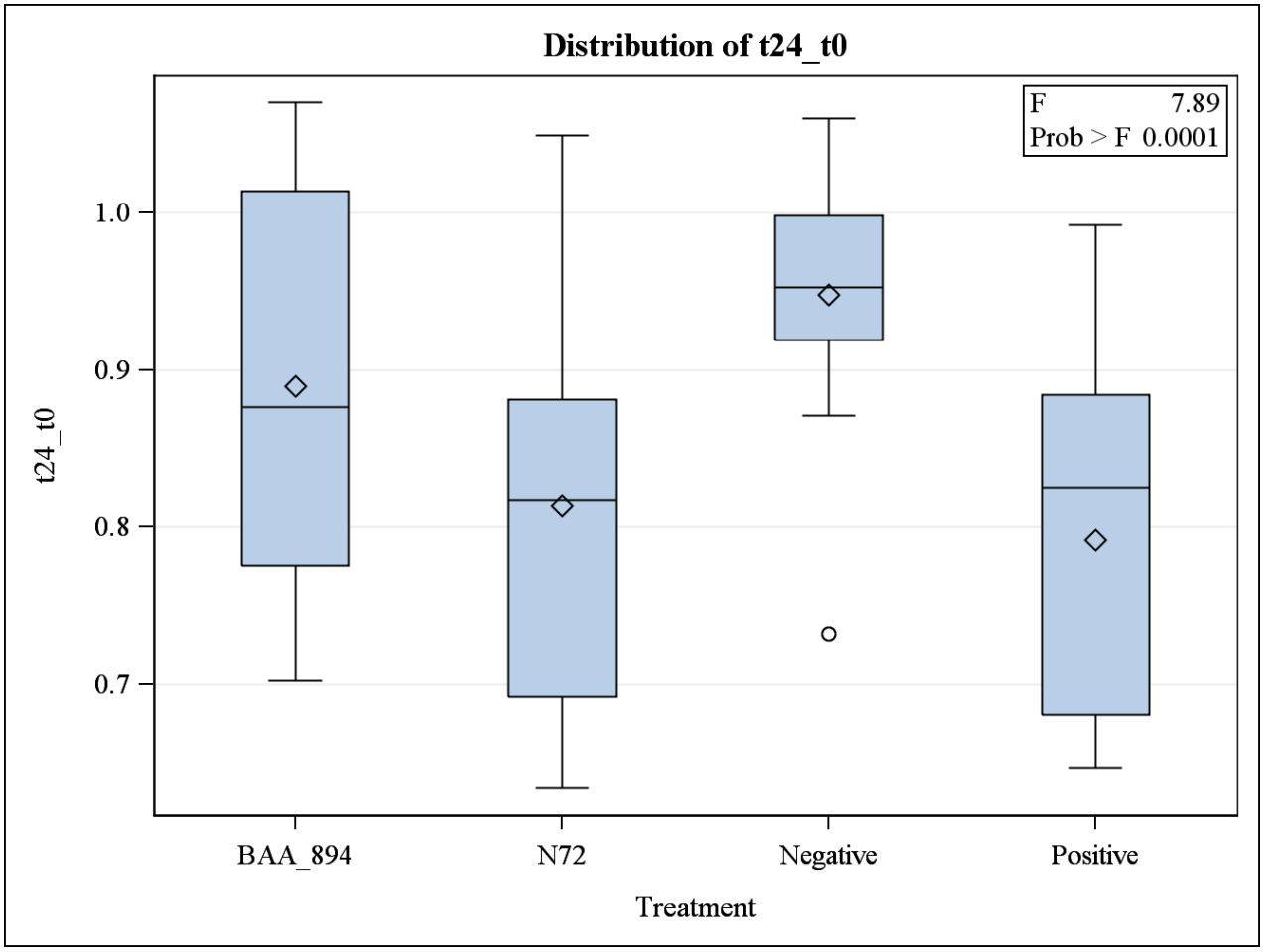

Figure A2. Distribution %Δhour 0-24.

Treatment	%ΔH0-24 LSMEAN	LSMEAN Number
BAA-894	0.88943485	1
N72	0.81334303	2
Negative	0.94778657	3
Positive	0.79217072	4

Least Squares Means for effect Treatment Pr > |t| for H0: LSMean(i)=LSMean(j) Dependent Variable: %ΔH0-24				
i/j	**1**	**2**	**3**	**4**
1		0.1583	0.3735	0.0415
2	0.1583		0.0020	0.9355
3	0.3735	0.0020		0.0003
4	0.0415	0.9355	0.0003	

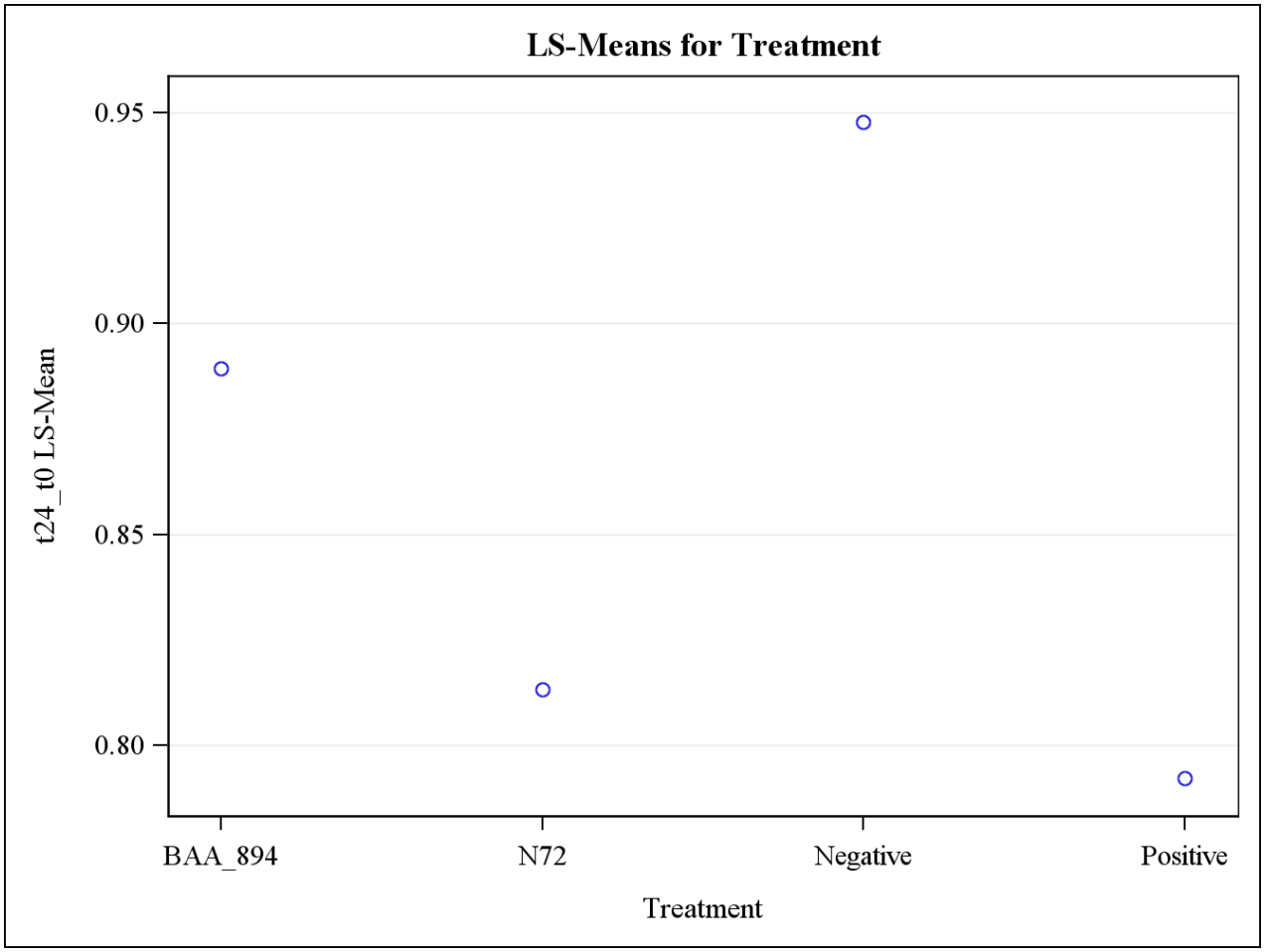

Figure A3. LS means data for treatment (%Δhour 0-24).

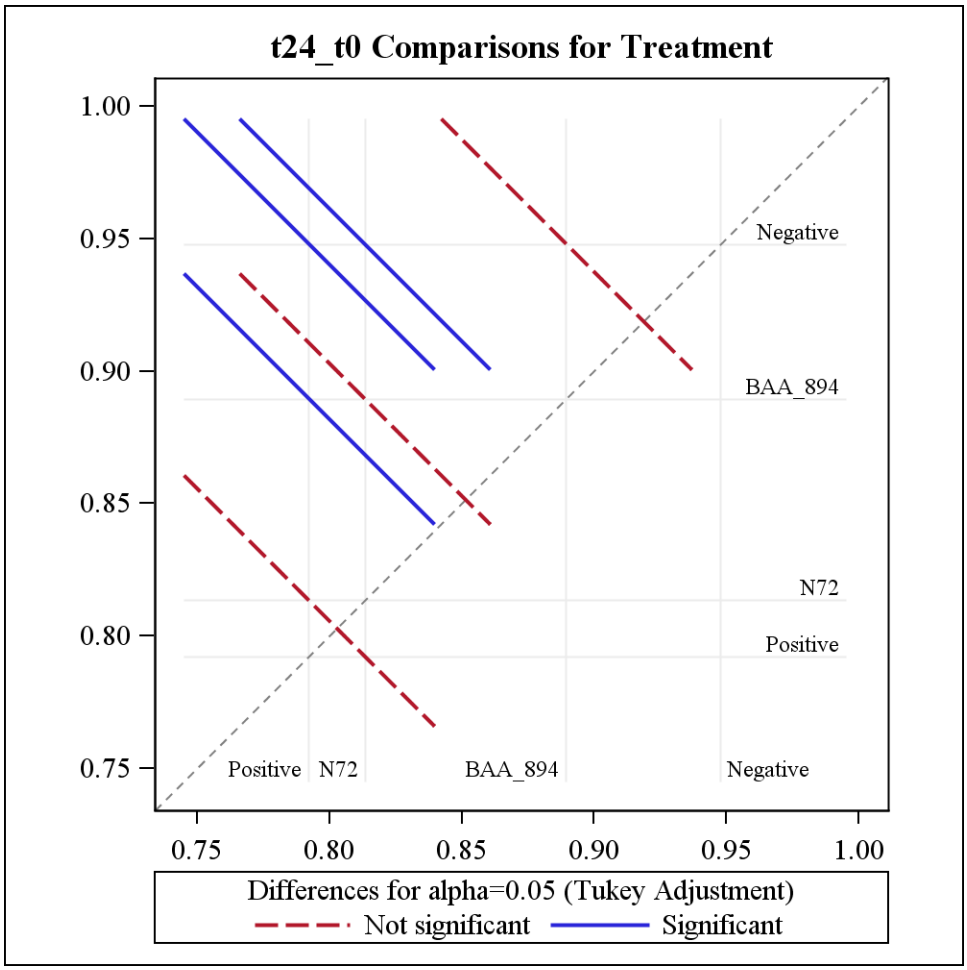

Figure A4. Comparison for treatment (%Δhour 0-24).